MCR-72-324

ABLATIVE AND METALLIC HEAT SHIELDS

FOR AEROBRAKING REENTRY

<u>TASK B-1 REPORT</u>

December, 1972

Contract NAS8-27161

MARTIN MARIETTA AEROSPACE
Denver Division
P. O. Box 179
Denver, Colorado 80201

MCR-72-324

Ablative and Metallic Heat Shields

for Aerobraking Reentry

Task B-1 Report

December, 1972

Contract No. NAS8-27161

Approved by:

Eric L. Strauss

Eric L. Strauss
Program Manager

MARTIN MARIETTA AEROSPACE
Denver Division
P. O. Box 179
Denver, Colorado 80201

FOREWORD

This report is submitted in compliance with Phase II, Task 5 (Reports) of Exhibit A, Scope of Work, dated 29 June 1972 for Contract NAS8-27161.

Phase II of the Contract consists of five Tasks:

    Task I: Test Environment and Model Definition

    Task II: Model Design and Fabrication

    Task III: Ablator Test and Evaluation

    Task IV: Conference Requirement

    Task V: Reports

This report documents the studies performed under Task I: "Test Environment and Model Definition".

TABLE OF CONTENT

LIST OF TABLES

LIST OF FIGURES

List of Figures (Continued)

List of Figures (Concluded)   <u>Page</u>

MCR-72-324

I. INTRODUCTION

The objectives of this study were to establish the feasibility of utilizing ablative or metallic heat shields for aerobraking reentry and to ascertain realistic ablative heat shield weights and design criteria for both ablative and metallic heat shields.

The ablative and metallic heat shields were for application to a 14 ft-diameter cylindrical body entry configuration with a 2:1 elliptical dome. Both a low drag and high drag configuration were studied. The high drag would be achieved by attachment of a 60° flare at the aft end of the cylinder (see Figure 1). The aerobraking trajectory pertained to the transfer of the vehicle from a geosynchronous orbit to the orbit of the Space Shuttle. Aerobraking trajectories involving two perigee passes and 30 perigee passes were investigated.

In the performance of Task 1, "Test Environment and Model Definition", the following was accomplished:

1. Test parameters and criteria for aerobraking heat shields were established with respect to stagnation point heating rate, heat flux distribution, pressure, enthalpy, space flight between entry passes, safety factors, initial temperatures and materials selection.

2. Ablative heat shield requirements were determined as a function of total heat input. Temperatures and pyrolysis depths were calculated as a function of time for stagnation point and off stagnation point locations pertaining to both low drag and high drag configurations flying two-pass and 30-pass aerobraking trajectories.

3. Metallic heat shield temperatures were calculated as a function of time for stagnation point and off stagnation point locations of low drag and high drag configurations flying the 30-pass entry trajectory.

4. One and two step plasma arc test pulses were selected which simulated pertinent flight environment parameters. Peak heating rate, total exposure time, total integrated heat flux, enthalpy and pressure were simulated for ablative models and time at temperature and pressure were simulated for the metallic heat shield models.

MCR-72-324

II. TEST PARAMETERS AND CRITERIA

Test parameters and criteria were primarily based on data from References 1 and 2. Stagnation point heating rate data from Reference 2 are reproduced in Figures 2, 3 and 4 as follows:

Figure 2 - Heating Rate History for Low Drag Configuration - 2-Pass Aerobraking Entry

Figure 3 - Heating Rate History for High Drag Configuration - 2-Pass Aerobraking Entry

Figure 4 - Heating Rate History for High Drag Configuration - 30-Pass Aerobraking Entry

For purposes of computer analyses, these heating pulses were converted into analogous pulses represented by a series of straight lines as shown in Figures 5, 6 and 7. The heat flux distribution over a 2:1 ellipse is shown in Figure 8. Peak heating rates and the corresponding radiation equilibrium temperatures (based on $\epsilon = 0.9$) for selected locations on the elliptical dome are summarized in Table 1. Heating rate values for the low drag configuration with 30 entry passes were obtained by multiplying the corresponding heating rates for the high drag configuration by a factor of 1.63.

The pressure distribution over the elliptical nose is shown in Figure 9. The maximum stagnation pressure is 152 lb/ft^2 (.139 atm) for the 2-pass trajectory and 15.9 lb/ft^2 (.013 atm) for the 30-pass trajectory.

The cold wall heating rate data (Figures 5, 6 and 7) along with the time histories of altitude and velocity (Figures 10 through 15) were input data to the Martin Marietta Corporation TCAP Ablation Program which computes hot wall heating rates and enthalpies as follows:

$$\dot{q}_{hw} = \dot{q}_{cw} \left(\frac{H_R - H_W}{H_R} \right)$$

$$H_R = \frac{V^2}{2gJ} + H_{\infty}$$

where: H_R = Recovery enthalpy

H_W = Enthalpy of the hot wall

V = Velocity

J = Mechanical equivalent of heat

H_∞ = Free stream enthalpy

Laminar flow was assumed throughout in conjunction with the 1959 Model Atmosphere. Free molecular heating was considered above 350,000 ft and considered as a cold wall heat flux term. Aerodynamic heating was insignificant above 450,000 ft and was therefore neglected. The calculated recovery enthalpies are summarized below:

High Drag Configuration - 2-Pass Trajectory

Pass 1 - 20,870 BTU/lb

Pass 2 - 17,290 BTU/lb

High Drag Configuration - 30-Pass Trajectory

Pass 1 - 20,950 BTU/lb

Pass 15 - 17,780 BTU/lb

Pass 30 - 13,000 BTU/lb

Low Drag Configuration - 2-Pass Trajectory

Pass 1 - 19,900 BTU/lb

Pass 2 - 16,950 BTU/lb

For the High Drag Configuration, the duration of the two pass entry mission is approximately 32,000 sec (.37 days). This represents the time from synchronous orbit to the apogee after the second entry pass. The corresponding duration of the 30 pass entry mission is 468,000 sec (5.43 days). The interval between entry heating (410,000 ft altitude outleg to 410,000 ft altitude inleg of the succeeding pass) for the high drag configuration is as follows:

2-Pass Trajectory

Pass 1 to Pass 2 - 12,100 sec

MCR-72-324

30 Pass Trajectory

Pass 1 to Pass 2 - 34,170 sec

Pass 15 to Pass 16 - 12,960 sec

Pass 29 to Pass 30 - 5,540 sec

A temperature of $1r)°F$ was assumed for the heat shield and backup structure at time of first entry. Cooldown after the first entry was calculated with one-half solar constant (.0611 BTU/ft^2-sec) applied to the exterior of the heat shield. The heat shield and backup structure stabilized to an equilibrium temperature of approximately 175°F in less than the coast time. A temperature of 175°F was therefore used as the initial temperature at entry for all passes except the first entry pass.

No uncertainty factors or safety factors were applied to the heating rate histories. The vehicle was assumed to enter at a zero angle of attack. It should be recognized that atmospheric dispersions can raise maximum equilibrium temperatures about 75°F. Similarly, a 10% decrease in surface emissivity will raise the maximum equilibrium temperature approximately 80°F.

The aluminum dome structure for the ablative heat shields is shown in Figure 16. An equivalent skin thickness was calculated which combined the mass of the aluminum skin and stiffeners. In the stagnation region, the equivalent aluminum skin thickness was 0.156 in. The equivalent aluminum skin thickness for off stagnation point regions was 0.083 in. The ablative heat shields must limit the aluminum structure to a maximum temperature of 300°F. In thermal analyses, the inner surface of the aluminum structure is treated as an adiabatic wall.

Silicone-base ablators were selected as the heat shield materials because of their low temperature flexibility, ease of application, and their proven performance in flight and ground simulation testing of vehicles such as PRIME, PAET, Viking and Space Shuttle. Specifically, three Martin Marietta ablators were considered:

ESA-5500; 55 lb/ft^3 density

ESA-3560; 30 lb/ft^3 density

SLA-561; 15 lb/ft^3 density

Pertinent thermal and mechanical properties of these ablators are listed in Table 2.

The following criteria were used for selecting ablatives for plasma arc evaluations:

1. Minimum heat shield weight for limiting aluminum dome temperature to $300^\circ F$ maximum;

2. No surface recession or mechanical erosion of ablator char.

Char mass loss rates for ESA 5500 and ESA 3560 are shown in Figure 17. The recession threshhold for SLA-561 is shown in Figure 18. On the basis of these criteria, ablators were chosen for analysis and evaluation as follows:

Two Pass Entry - Low Drag Configuration

127 BTU/ft^2-sec peak heating rate

.139 atm peak stagnation pressure

ESA 5500

ESA 3560

Two Pass Entry - High Drag Configuration

85 BTU/ft^2-sec peak heating rate

.139 atm peak stagnation pressure

ESA 3560

SLA-561

Thirty-Pass Entry - High Drag Configuration

21.55 BTU/ft^2-sec peak heating rate

.013 atm peak stagnation pressure

ESA 3560

SLA-561

Metallic heat shields were selected for the thirty-pass entry trajectories only. Haynes 188 will be evaluated for temperatures of 1700° to $2000^\circ F$. Above $2000^\circ F$, FS-85 columbium alloy with a silicide coating (R512E) is the material of choice. Specifically, the columbium alloy will be evaluated for the temperature range of 2300° to $2600^\circ F$.

III. ABLATIVE HEAT SHIELD REQUIREMENTS

Design curves for ablator thickness were generated for two pass and
30 pass entries. For the two pass mission, ablation and heat transfer
were calculated by means of the TCAP Ablation Program for the entry
heat pulses and the ensuing space flight. The computations were con-
tin...d until the temperature of the aluminum structure peaked after
the second entry pass. Analyses were performed for 100%, 50% and 10%
of stagnation point heating. The runs conducted and the results obtained
are summarized in Table 3. Ablator thickness requirements for a 300°F
backface (aluminum) temperature were established by interpolation or
extrapolation from the data points of Table 3. This is illustrated in
Figure 19. The resulting ablator thicknesses and ablator weights are
tabulated below:

Low Drag Configuration

ESA 5500 Ablator

.156 Aluminum Thickness

100% Heating - 2.08 in. (9.53 lb/ft^2)

50% Heating - 1.60 in. (7.33 lb/ft^2)

.083 Aluminum Thickness

100% Heating - 2.25 in. (10.30 lb/ft^2)

50% Heating - 1.75 in. (8.02 lb/ft^2)

ESA 3560 Ablator

.156 Aluminum Thickness

100% Heating - 1.43 in. (3.58 lb/ft^2)

50% Heating - 1.14 in. (2.86 lb/ft^2)

.083 Aluminum Thickness

100% Heating - 1.52 in. (3.80 lb/ft^2)

50% Heating - 1.27 in. (3.18 lb/ft^2)

10% Heating - 0.87 in. (2.18 lb/ft^2)

High Drag Configuration

ESA 3560 Ablator

.156 Aluminum Thickness

100% Heating - 1.36 in. (3.40 lb/ft^2)

50% Heating - 1.04 in. (2.60 lb/ft^2)

.083 Aluminum Thickness

    100% Heating - 1.46 in. (3.65 lb/ft^2)

    50% Heating - 1.22 in. (3.05 lb/ft^2)

    10% Heating - 0.79 in. (1.98 lb/ft^2)

SLA-561 Ablator

  .156 Aluminum Thickness

    100% Heating - 1.68 in. (2.06 lb/ft^2)

    50% Heating - 1.25 in. (1.53 lb/ft^2)

    10% Heating - 0.57 in. (0.70 lb/ft^2)

  .083 Aluminum Thickness

    100% Heating - 1.68 in. (2.06 lb/ft^2)

    50% Heating - 1.38 in. (1.69 lb/ft^2)

    10% Heating - 0.75 in. (0.92 lb/ft^2)

Typical curves showing surface and backface (aluminum) temperatures vs time are presented in Figures 20 and 21. Temperature distributions through a typical ablator at time of peak surface temperature for the two heat pulses are shown in Figure 22.

A continuous computer analysis of the 30 pass trajectories including entry heating and space flight would be impractical because of the length and complexity of the computer runs. Therefore, three average heat flux curves were developed as shown in Figure 23 and used in the analysis as the heating rate input. Also, since the two pass analysis had shown that the ablator and backup structure reach an equilibrium temperature of approximately 175°F between entry passes, the computations were shortened as follows:

1. Analysis was performed for each heating cycle with the initial portion of cooldown (100-200 sec) until cessation of pyrolysis.

2. Initial conditions for each subsequent heating cycle were the depth of char and pyrolysis zone from the previous entry pass and a temperature of 175°F.

3. Analysis of cooldown for the 30th entry pass was continued until the temperature of the aluminum structure reached its peak value.

To determine design ablator thicknesses, the analyses were first performed for an infinitely thick ablator slab and the thickness of the char layer and depth of the pyrolysis zone were determined. Figure 24 shows the progression of the char and pyrolysis zone layers for the thirty entry pulses. At the conclusion of the thirtieth entry pass, ablator degradation had progressed to the following depths:

	Char Thickness (in.)			Char & Pyrolysis Zone (in.)		
Percent of Stagnation Point Heating	100	50	10	100	50	10
ESA 3560	1.08	0.68	0.02	1.36	0.94	0.22
SLA-561	0.54	0.62	0.02	0.98	0.98	0.24

Using the char thickness and pyrolysis zone at the end of the 24th pass as initial conditions, passes 25 through 30 were then rerun for various ablator thicknesses as summarized in Table 4. In some instances, only the thirtieth pass was run with the char thickness and pyrolysis zone at the end of the 29th pass as the initial condition. Ablator thicknesses for a $300°F$ aluminum temperature were established by interpolation or extrapolation from these data points as illustrated in Figure 25. The resulting ablator thicknesses and ablator weights are tabulated below:

High Drag Configuration

ESA 3560 Ablator

.156 Aluminum Thickness

100% Heating - 2.13 in. (5.35 lb/ft^2)

10% Heating - 0.72 in. (1.81 lb/ft^2)

ESA 3560 Ablator

.083 Aluminum Thickness

100% Heating - 2.19 in. (5.50 lb/ft^2)

50% Heating - 1.82 in. (4.55 lb/ft^2)

10% Heating - 0.85 in. (2.13 lb/ft^2)

SLA-561 Ablator

.156 Aluminum Thickness

100% Heating - 1.92 in. (2.35 lb/ft^2)

SLA-561 Ablator

.083 Aluminum Thickness

100% Heating - 2.09 in. (2.56 lb/ft^2)

50% Heating - 1.40 in. (1.72 lb/ft^2)

10% Heating - 0.77 in. (0.94 lb/ft^2)

Ablator design curves for the two pass and thirty pass entry missions shown in Figures 26 and 27 are plots of ablator thickness (for 300°F aluminum temperature) vs total integrated heat flux. These curves must be considered as preliminary design curves since they have been constructed from a maximum of three data points (100%, 50% and 10% of stagnation point heating). However, these curves are useful for estimating total ablative heat shield weights for the elliptical dome section.

IV. METALLIC HEAT SHIELD TEMPERATURES

Temperature histories for metallic heat shields were calculated for the thirty pass entry trajectories. The analytical model consisted of 0.029 inch thick Haynes 188 sheet with an emissivity of 0.80 and backed up by 1.56 inch of thermal insulation. A 0.156 inch thickness of aluminum in back of the insulation represented the internal heat sinks within the elliptical dome. Temperatures were calculated for three locations on the dome - the stagnation point and points "B" and "C" of Figure 1 - and are shown in Figures 28, 29 and 30 respectively for both high drag and low drag configurations. Calculated peak temperatures are lower than equilibrium temperatures since they are based on the heat transfer to the hot wall and also account for the heat loss through the insulation to the aluminum heat sink. Calculated peak temperatures are listed below:

Low Drag Configuration

Point "A"

Pass 1 - 2210°F
Pass 15 - 1820°F
Pass 30 - 1830°F

Point "B"

Pass 1 - 2100°F
Pass 15 - 1720°F
Pass 30 - 1720°F

Point "C"

Pass 1 - 670°F
Pass 15 - 500°F
Pass 30 - 550°F

High Drag Configuration

Point "A"

Pass 1 - 1840°F
Pass 15 - 1660°F
Pass 30 - 1740°F

Point "B"

Pass 1 - 1740°F
Pass 15 - 1570°F
Pass 30 - 1640°F

Point "C"

Pass 1 - 490°F
Pass 15 - 430°F
Pass 30 - 510°F

V. PLASMA ARC TEST PULSE SELECTION

Plasma arc test pulses were selected consistent with the capabilities of the Martin Marietta Plasma Arc Facility. For ablative heat shield models, the plasma arc environment simulates the peak heating rates, total exposure times and total heats of entry heating at the stagnation point. The test pressures are approximately 50% of flight pressures at the stagnation point. The high flight enthalpies cannot be simulated in the plasma arc. Simulation of two pass entry heating is accomplished with a 3-in. diameter exit nozzle, while simulation of 30 pass entry heating can be accomplished with a 10-in. diameter exit nozzle. Plasma arc test pulses simulating two pass-stagnation point heating for the Low Drag Configuration are shown in Figure 31. Similar test pulses for the High Drag Configuration are shown in Figure 32. The degree of simulation is illustrated below:

	Entry Heating	Test Pulse
Low Drag Configuration		
Peak Heating Rate - Pulse 1	127	120
(BTU/ft^2-sec) Pulse 2	94	80
Total Heat - Pulse 1	11,590	11,250
(BTU/ft^2) Pulse 2	16,950	17,100
High Drag Configuration		
Peak Heating Rate - Pulse 1	86	80
(BTU/ft^2-sec) Pulse 2	63	55
Total Heat - Pulse 1	9,950	9,500
(BTU/ft^2) Pulse 2	11,740	12,650

Ablation analysis was performed for a 1.43 inch-thick ESA 3560 model subjected to the Low Drag Configuration test pulse. In the analysis, the changes in heating rate were allowed to occur over a 20 to 30 second interval rather than instantaneously. The initial temperature at start of test was assumed to be $80°F$. The time interval between model insertion for the first and second heat pulses was programmed to be 4000 secs. In between heat pulses, the model was allowed to cool by letting its front face radiate to the $100°F$ wall of the plasma arc tank. The inner surface of the aluminum backface was assumed to be adiabatic. Time-temperature plots for the surface and backface are shown in Figure 33. It can

be seen that temperatures tended to stabilize at approximately 150°F
during the cooldown period. The aluminum temperature began to exceed the
surface temperature at approximately 2100 seconds after start of heating.
Thereafter, the temperature difference within the model did not exceed
14°F.

To arrive at test pulses for the 30 pass ablator models, the peak
heating rates, total heats and pulse durations were first estimated for
each pulse by drawing a smooth curve through the known data points for
passes 1, 15 and 30 as shown in Figure 34. The total heat for all 30
passes as determine. from Figure 34 is 86,480 BTU/ft^2. Test pulses were
then established as shown in Figure 35. Pulses 1 through 4 and 28 through
30 are two step pulses simulating peak heating, rate, total heat and pulse
duration for the flight environment. The remaining pulses are single
step pulses and simulate total heat and pulse duration only. In a second
series of test runs, the first fifteen pulses of the thirty pass entry
trajectory were to be simulated by a series of two step pulses as shown
in Figure 36. The degree of simulation achieved is illustrated below:

		Entry Heating	30 Pass Test Series	15 Pass Test Series
Peak Heating Rate -	Pulse 1	22.0	20.0	20.0
(BTU/ft^2-sec)	Pulse 15	18.5	-	15.0
	Pulse 30	16.0	14.0	-
Total Heat	- Pulse 1	2,320	2,290	2,290
(BTU/ft^2)	Pulse 15	2,120	2,640	2,280
	Pulse 30	5,600	5,100	-
	Pulse 1 through 15	33,190	-	33,250
	Pulse 1 through 30	86,480	87,300	-
Pulse Duration	- Pulse 1	225	230	230
(sec)	Pulse 15	300	330	260
	Pulse 30	750	650	-

Plasma arc testing of the ablator models shall be conducted in accor-
dance with the following procedures:

1. All test points shall be calibrated for heating rate, enthalpy
and stagnation pressure. Heating rate calibration shall use a calorimeter
of the same diameter as the model. The time required to change from the
high heating rate to the low heating rate conditions of dual pulses shall
be reported. In the "two pass" heating tests, heating rate and stagna-
tion pressure of each test point shall be calibrated for each test. In
the 30 and 15 pass heating tests, heating rate and stagnation pressure
of each test point shall be calibrated periodically during the test.

2. Internal temperatures shall be recorded during the heating and cooling portions of the tests. In addition, surface temperature at the stagnation point shall be recorded. Specimens shall be allowed to cool between passes until internal thermocouples are within 20°F of one another. Temperatures after last pass shall be recorded until thermocouple on aluminum backface reaches its maximum temperature. Motion picture coverage of the plasma arc exposures shall be obtained at a rate of one frame per second. All temperature data shall be provided as plots of temperature vs time. All calibration data and arc operating conditions shall be provided in tabular form.

3. Specimens shall be photographed after testing. A description of the specimen appearance, especially the condition of the surface, shall be given. Surface recession, if any, shall be measured. Thereafter, the specimens shall be sectioned and the following shall be measured:

> Total ablator plus char thickness;
>
> Char thickness;
>
> Char plus pyrolysis zone thickness;
>
> Virgin ablator thickness.

Model cross-section shall be photographed and all anomalies (cracks, voids, etc) shall be noted.

Plasma arc test pulses for metallic heat shields were selected to simulate temperature rather than heat flux. Test pulses were based on the temperature histories for metallic heat shields shown in Figures 28 and 29. One set of test pulses was selected for columbium models to simulate stagnation temperatures for the Low Drag Configuration. Figure 37 shows how the test pulses were derived from the temperature histories. A "lower boundary" temperature was selected which approximates the peak hot wall temperature. The "upper boundary" temperature is 300°F higher than the "lower boundary" temperature and accounts for possible temperature increases due to atmospheric dispersions, flight trajectory variations and surface emissivity changes. An intermediate temperature, 200°F higher than the "lower boundary" temperature, was selected as an additional test series. The lengths of the test pulses was chosen to correspond to the time periods in the flight temperature history when the hot wall temperature exceeds 67% of the peak temperature value for the particular entry pass. Figure 38 shows the complete series of plasma arc test pulses.

A second set of test pulses was selected for Haynes 188 models to simulate Point "B" temperatures for the High Drag Configuration. The derivation of the test pulses shown in Figure 39 is analogous to that for the columbium models except that the intermediate temperature is

$150°F$ higher than the "lower boundary" temperature. The complete series of plasma arc test pulses is shown in Figure 40.

Simulation of these temperature environments can be accomplished with a 6-inch diameter exit nozzle. A stagnation pressure of 0.010 atmospheres and a stream enthalpy of approximately 5000 BTU/lb is projected.

Plasma arc testing of metallic heat shield models shall be conducted in accordance with the following procedures:

1. The cold wall heat flux rates which will produce the specified surface temperatures shall be calculated. Test points shall be calibrated for these heating rates; however, during the test runs, power to the arc shall be adjusted to attain the required temperatures within $\pm 25°F$. A thermocouple located at the model stagnation point shall be monitored to assure that the model temperature requirements are met.

2. Each model shall be cycled through the 30 pulses consecutively before the next model is tested. The lowest temperature condition shall be tested first and the highest temperature condition shall be tested last. After each test pulse, the model may be reinserted into the test stream when the surface temperature has dropped below 50% of the specified surface temperature. In case of failure (burn-through), testing shall be halted and the failed model shall be removed from the plasma arc for examination. The severity of the test environment for untested models may then be reduced as determined by the Program Manager.

3. All test points shall be calibrated for heating rate, enthalpy and stagnation pressure. Heating rate calibration shall use a calorimeter of the same diameter as the model. Calibrations shall be performed periodically during the 30-pulse test run.

4. Thermocouple data shall be recorded during the heating and cooling portions of the tests. In addition, surface temperature at the stagnation point shall be monitored with a recording optical pyrometer. Motion picture coverage of the plasma arc exposures shall be obtained at the rate of one frame per second. All temperature data shall be provided as plots of temperature vs time. All calibration data and arc operating parameters shall be provided in tabular form.

5. After testing, specimens shall be photographed to document surface appearance, discolorations, oxidation and coating failure. A description of the specimen appearance shall be given. Thermal distortions of the specimen shall be measured. Thereafter, a segment of the

metal shall be removed from the stagnation area and examined metallurgically. Grain structure and coating characteristics shall be compared to those of untested control materials or of material taken from the attachment tabs of the models.

VI. REFERENCES

1. "Space Tug Aerobraking Study - Status Report", prepared under Contract NAS8-27501, The Boeing Company, Huntsville, Alabama.

2. C. J. Corso and C. L. Eger, "Space Tug Aerobraking Study" - Volume II of II, Technical Volume. Beoing Document No. D5-17142, prepared under Contract NAS8-27501, The Boeing Company, Huntsville, Alabama, April, 1972.

MCR-72-324

Table 1 - Peak Heating Rates and Equilibrium Temperatures

| Entry Pass | Heating Rate (BTU/ft^2-sec) | | | | | |
| | High Drag Configuration | | | Low Drag Configuration | | |
	Point "A"	Point "B"	Point "C"	Point "A"	Point "B"	Point "C"
	30-Pass Trajectory					
1	21.55	18.5	1.86	35.0	30.1	3.02
15	16.6	14.5	1.45	27.0	23.5	2.36
30	15.7	13.4	1.35	25.5	21.8	2.20
	2-Pass Trajectory					
1	85.0	73.0	7.30	127.0	109.0	10.90
2	63.0	54.1	5.42	94.0	80.7	8.08
	Equilibrium Temperature (°F)					
	30-Pass Trajectory					
1	2200	2100	980	2540	2425	1165
15	2030	1945	895	2360	2265	1070
30	1995	1900	870	2310	2200	1045
	2-Pass Trajectory					
1	3290	3140	1570	3680	3520	1790
2	3020	2890	1420	3380	3240	1620

Table 2 - Properties of Silicone Ablators

|	ESA-3560F	ESA-5500	SLA-561
Ablator Density (lb/ft^3)	30	55	15
Char Density (lb/ft^3)	10.5	30.9	8.3
Ablator Specific Heat (BTU/lb-$°F$)	0.26($70°F$)	0.19($70°F$)	0.30($70°F$)
Char Specific Heat (BTU/lb-$°F$)	0.37($1000°F$)	0.29($1000°F$)	0.37($1000°F$)
Ablator Thermal Conductivity (BTU/in-sec-$°R$)	1.3×10^{-6} ($300°F$)	3.0×10^{-6} ($300°F$)	0.7×10^{-6} ($300°F$)
Char Thermal Conductivity (BTU/in-sec-$°R$)	5.0×10^{-6} ($2500°F$)	9.5×10^{-6} ($2500°F$)	0.95×10^{-6} ($2500°F$)
Char Emissivity	0.80($2500°F$)	0.85($2500°F$)	0.92($2500°F$)
Specific Heat of Gaseous Products (BTU/lb-$°F$)	0.6	0.6	0.6
Heat of Depolymerization (BTU/lb)	0	0	0
Order of Decomposition Reaction	2	2	2
Fraction of Ablator that Vaporizes	0.65	0.44	0.44
Tensile Strength (psi)	150 ($70°F$) 350 ($-125°F$)	140 ($70°F$) 400 ($-125°F$)	60 ($70°F$) 150 ($-125°F$)
Tensile Elongation (%)	9.5 ($70°F$) 17.0 ($-125°F$)	36.0 ($70°F$) 60.0 ($-125°F$)	2.5 ($70°F$) 3.1 ($-125°F$)

Table 3 - Ablation Analyses for Two Pass Entry Missions

Ablation Material	% of Stagnation Heating	Aluminum Thickness (in.)	Ablator Thickness (in.)	Peak Aluminum Temperature (°F)	Peak Surface Temperature (°F)	Char Depth (in.)	Thickness of Char and Pyrolysis Zone (in.)
LOW DRAG CONFIGURATION							
ESA 5500	100	.156	1.70	345	-	-	-
			1.90	319	-	-	-
			2.05	304	2863	0.551	0.727
			2.16	292	-	-	-
ESA 5500	100	.083	2.16	307	2860	0.550	0.733
			2.30	296	-	-	-
ESA 5500	50	.156	1.60	307	2082	0.350	0.507
			1.72	286	-	-	-
ESA 5500	50	.083	1.70	306	2082	0.348	0.507
			1.96	276	-	-	-
ESA 3560	100	.156	1.40	304	3060	0.634	0.816
			1.50	286	-	-	-
ESA 3560	100	.083	1.55	296	3066	0.625	0.810
ESA 3560	50	.156	1.15	297	2393	0.446	0.622
ESA 3560	50	.083	1.30	296	2395	0.438	0.619
ESA 3560	10	.083	.65	345	-	-	-
ESA 3560	10	.083	.85	302	1204	0.057	0.232
HIGH DRAG CONFIGURATION							
ESA 3560	100	.156	1.25	313	2690	0.567	0.744
			1.70	246	-	-	-
ESA 3560	100	.083	1.50	294	2695	0.552	0.732
			1.60	278	-	-	-
ESA 3560	50	.156	.95	327	1979	0.374	0.546
			1.09	292	-	-	-
			1.30	259	-	-	-

(Continued)

Table 3 (Continued)

Ablation Material	% of Stagnation Heating	Aluminum Thickness (in.)	Ablator Thickness (in.)	Peak Aluminum Temperature (°F)	Peak Surface Temperature (°F)	Char Depth (in.)	Thickness of Char and Pyrolysis Zone (in.)
HIGH DRAG CONFIGURATION (Continued)							
ESA 3560	50	.083	1.05	346	-	-	-
			1.25	291	2000	0.365	0.557
			1.30	284	-	-	-
ESA 3560	10	.083	.65	336	-	-	-
			.80	298	1100	0.020	0.172
SLA-561	100	.156	1.65	305	2860	0.708	1.019
			1.75	292	-	-	-
SLA-561	100	.083	1.80	284	2954	0.703	1.021
			1.90	375	-	-	-
SLA-561	50	.156	1.23	303	2230	0.230	0.793
SLA-561	50	.083	1.10	360	-	-	-
SLA-561	10	.156	1.40	295	2332	0.515	0.807
SLA-561	10	.083	.58	299	1237	0.120	0.345
			.70	313	-	-	-
			.80	287	1185	0.094	0.355

Table 4 - Ablator Analyses for Thirty Pass Entry Missions

Ablation Material	Percent of Stagnation Heating	Aluminum Thickness (in.)	Ablator Thickness (in.)	Peak Aluminum Temperature (°F)	Peak Surface Temperature (°F)	Char Depth (in.)	Thickness of Char and Pyrolysis Zone (in.)
ESA 3560[1]	100	.156	4.80	176	-	0.958	1.246
ESA 3560[2]	100	.156	3.35	213	-	-	-
ESA 3560[2]	100	.156	2.90	235	-	-	-
ESA 3560[2]	100	.156	2.40	268	-	1.032	1.320
ESA 3560[2]	100	.156	2.00	328	-	-	-
ESA 3560[3]	100	.083	2.25	290	-	1.093	1.388
ESA 3560[3]	100	.083	2.05	322	-	-	-
ESA 3560[2,5]	50	.083	1.80	304	1595	0.681	0.944
ESA 3560[6]	10	.156	2.20	-	990	-	-
ESA 3560[2]	10	.156	1.00	251	-	-	-
ESA 3560[2]	10	.156	0.65	312	-	0.042	0.203
ESA 3560[3]	10	.083	0.80	309	-	0.042	0.201
SLA-561[2]	100	.156	2.10	271	-	0.924	1.353
SLA-561[4]	100	.156	1.90	-	2121	-	-
SLA-561[3]	100	.083	2.10	299	-	0.882	1.284
SLA-561[4]	50	.083	1.90	-	1690	-	-
SLA-561[2]	50	.083	1.50	282	-	0.619	0.989
SLA-561[4]	10	.083	1.90	-	1038	-	-
SLA-561[3]	10	.083	0.70	312	-	0.011	0.238

NOTES: [1]Pass 1 through 30; [2]Pass 25 through 30; [3]Pass 30; [4]Pass 1 through 11; [5]Pass 1 through 14; [6]Pass 1 through 24.

Figure 1 - Aerobraking Configuration Concepts
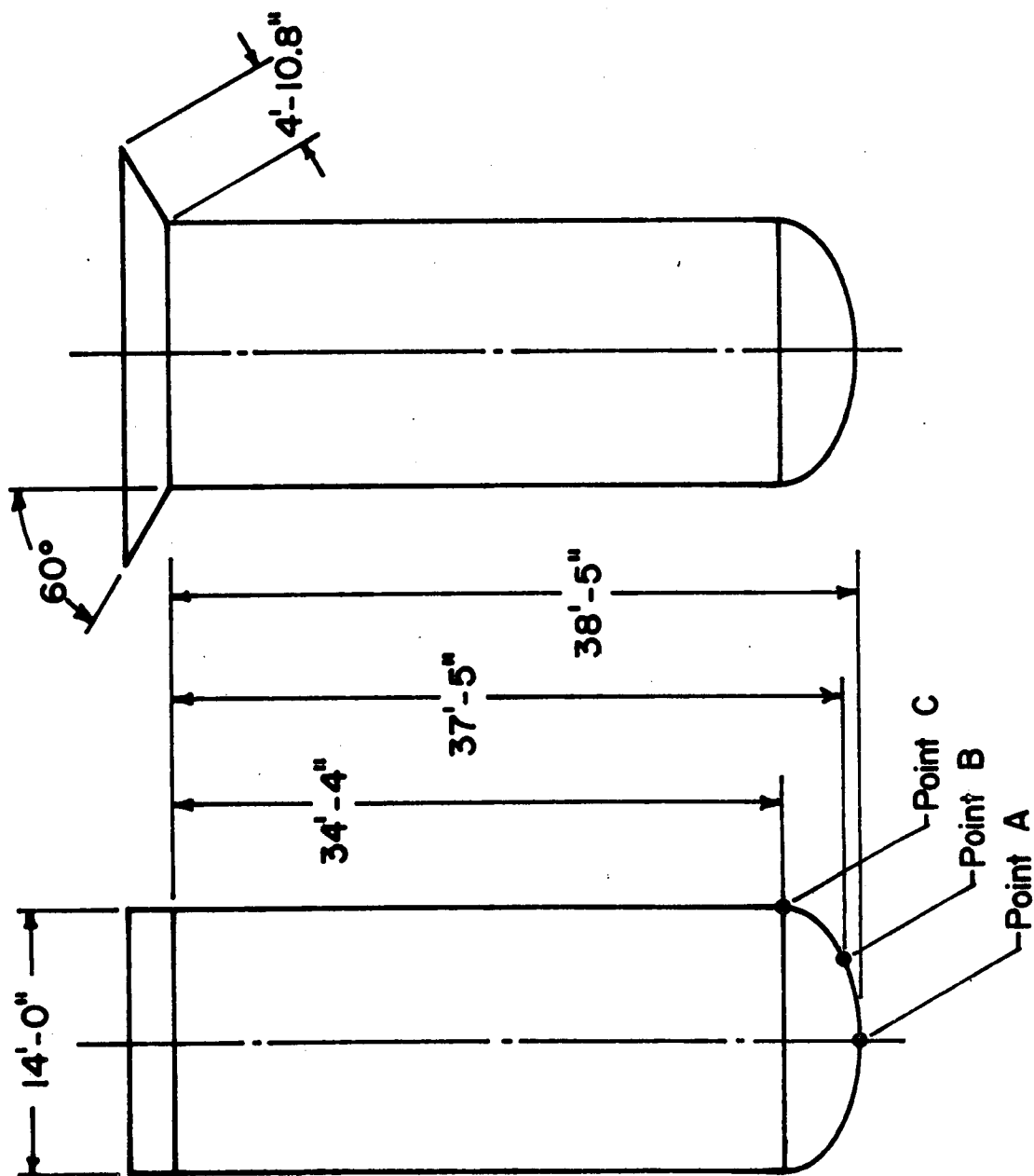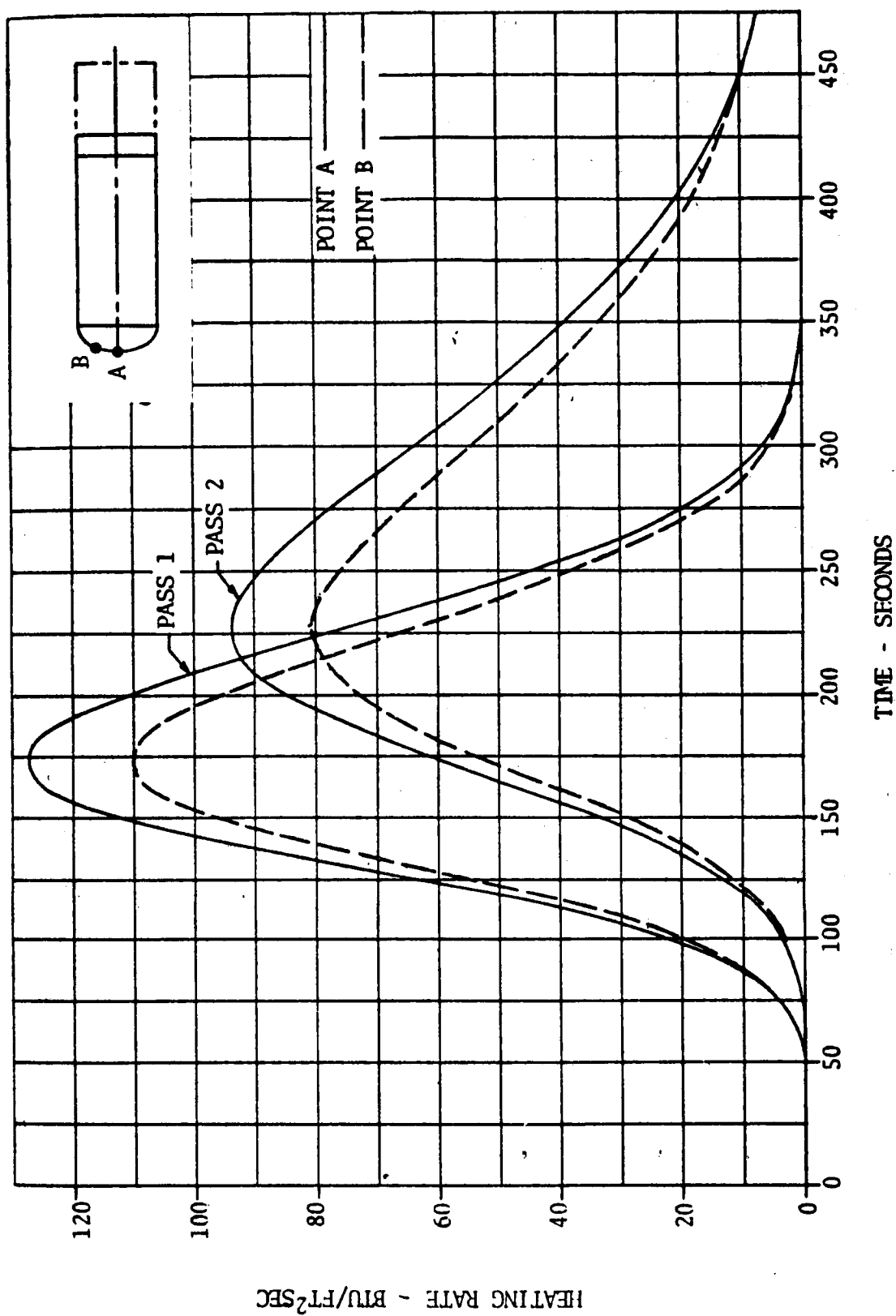
HIGH DRAG CONFIGURATION

LOW DRAG CONFIGURATION

4'-10.8"

60°

38'-5"

37'-5"

34'-4"

14'-0"

Point C

Point B

Point A

Figure 2 - Heating Rate History for Low Drag Configuration - 2 Pass Aerobraking Entry
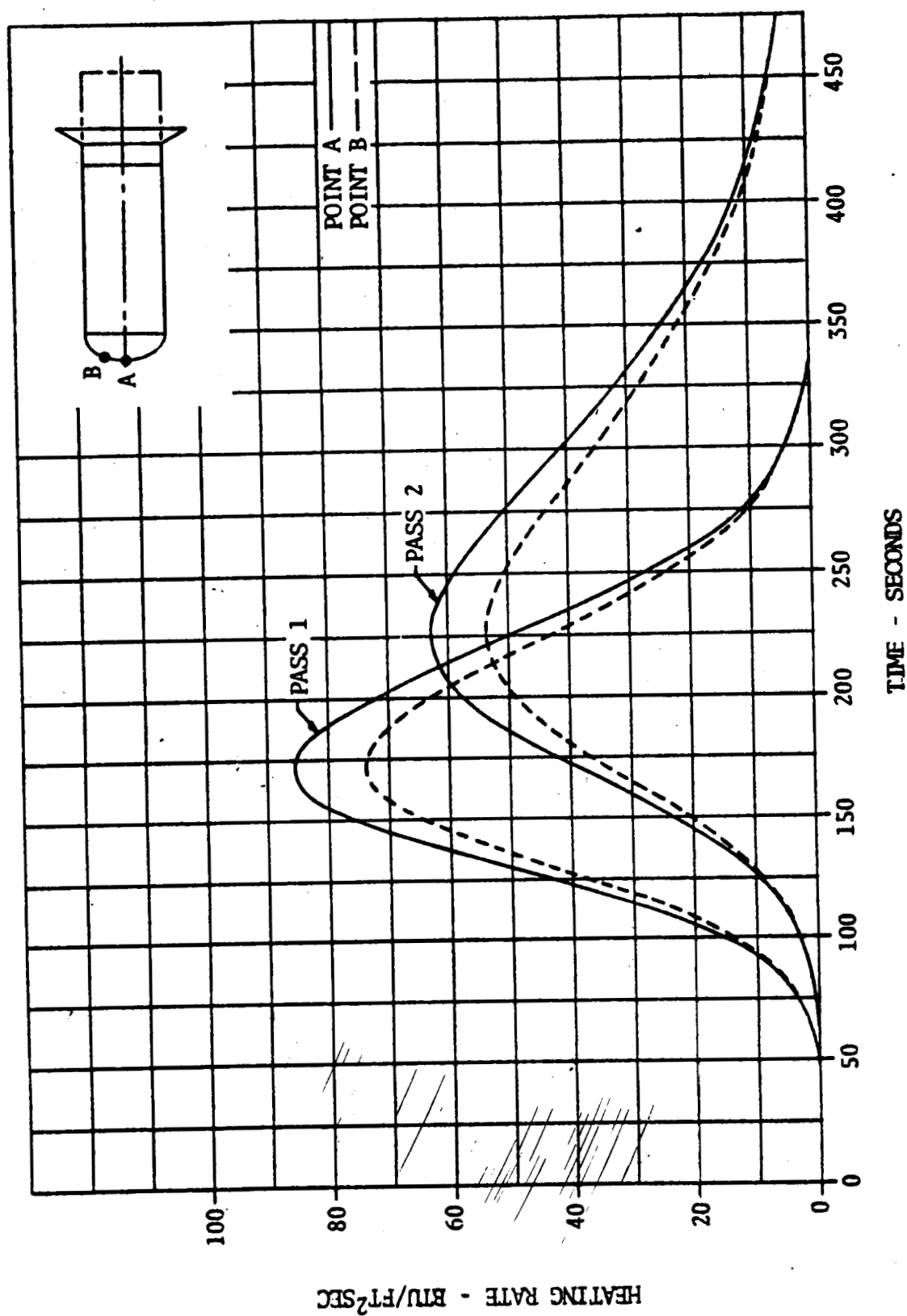
Figure 3 - Heating Rate History for High Drag Configuration - 2 Pass Aerobraking Entry
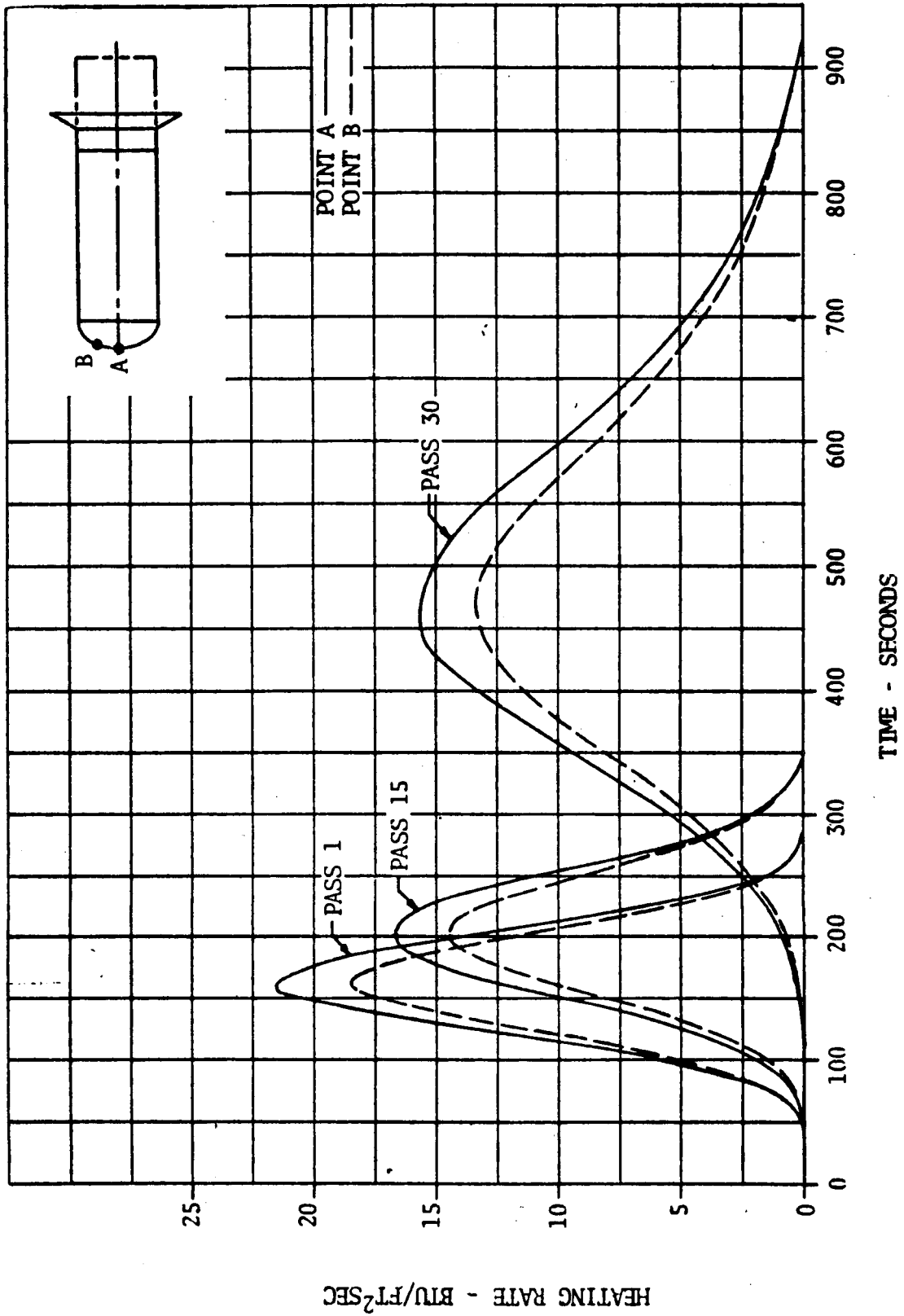
Figure 4 - Heating Rate History for High Drag Configuration - 30 Pass Aerobraking Entry
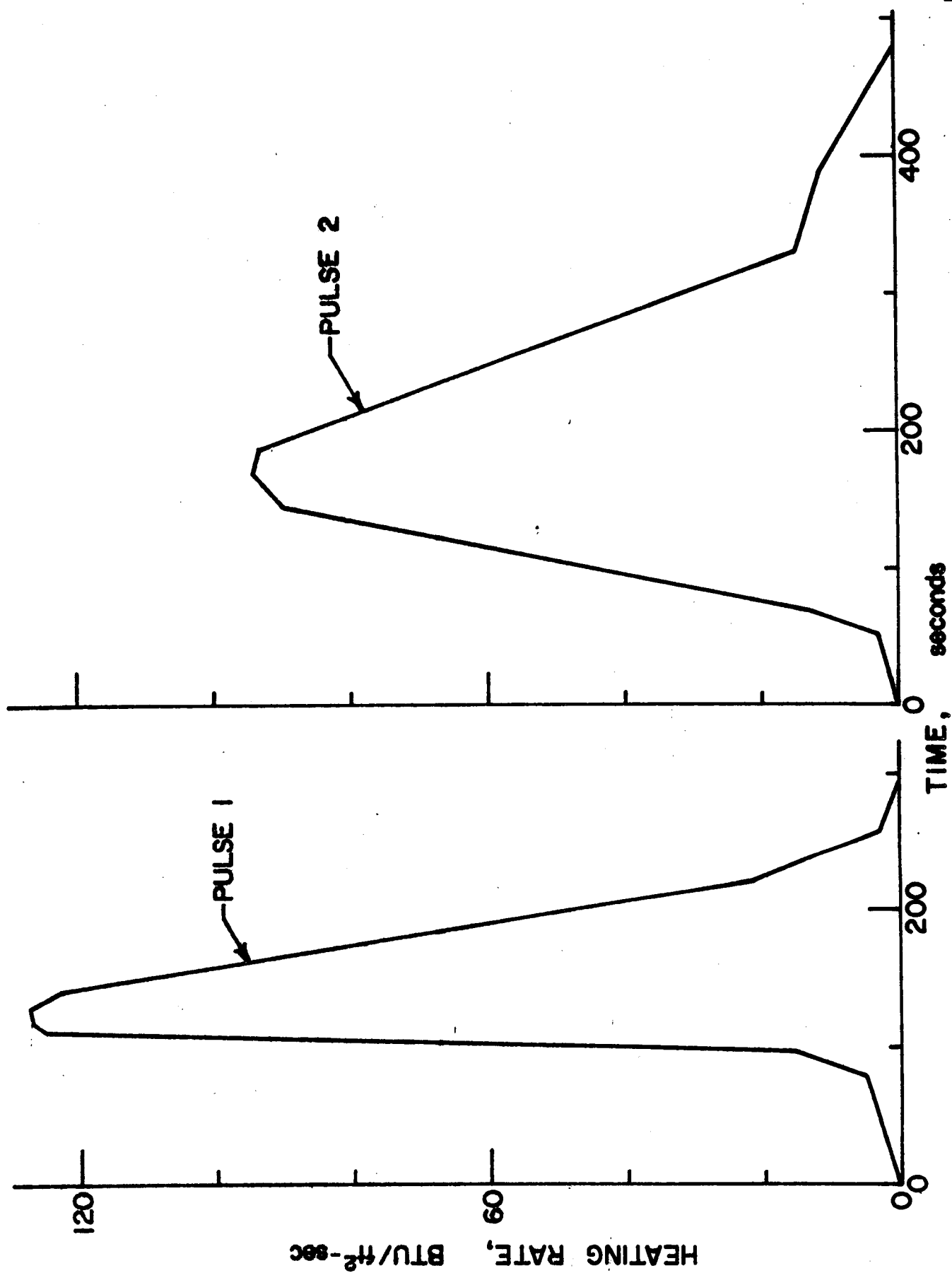
Figure 5 - Modified Heating Rate History for Low Drag Configuration - 2 Pass Aerobraking Entry
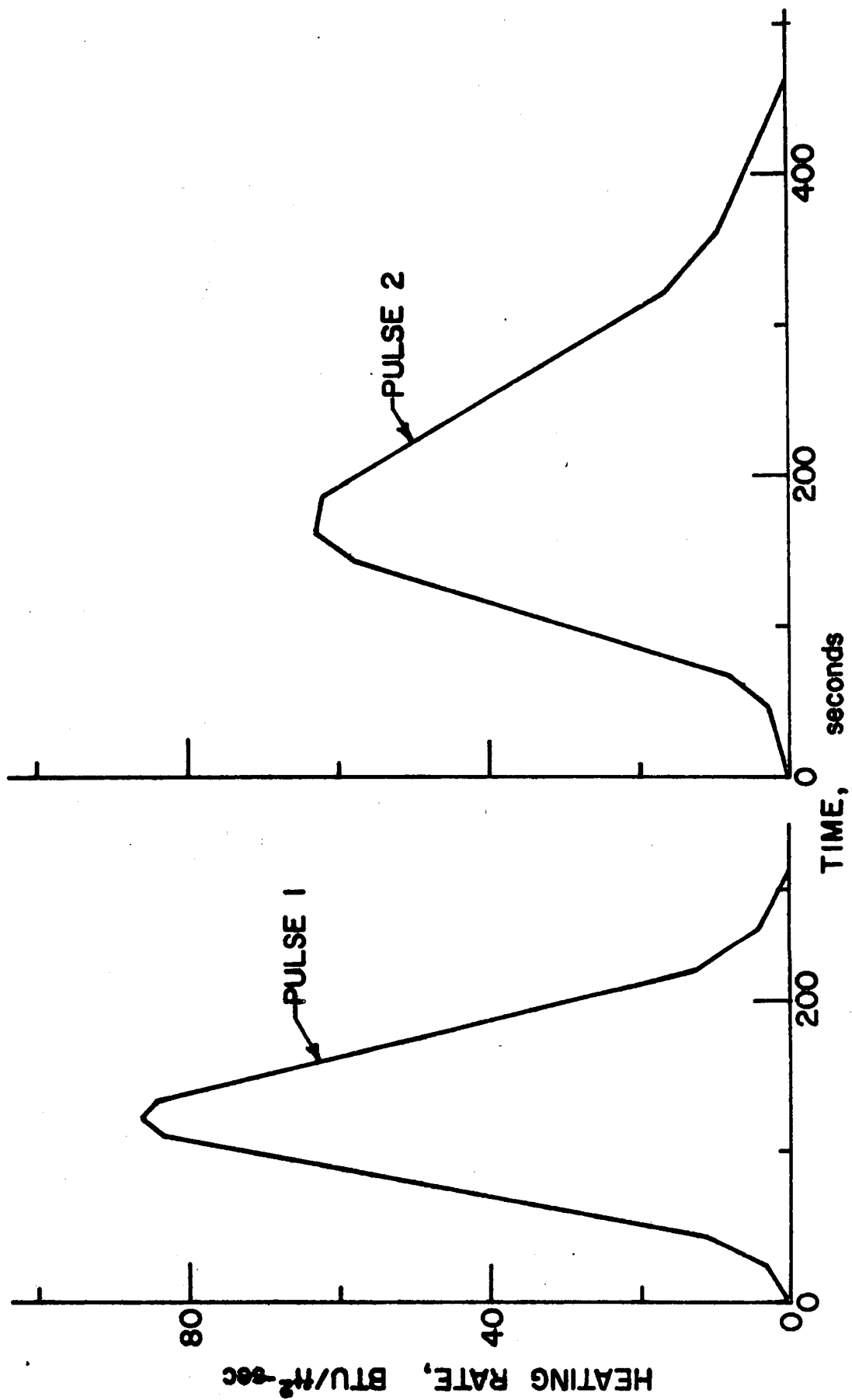
Figure 6 - Modified Heating Rate History for High Drag Configuration - 2 Pass Aerobraking Entry
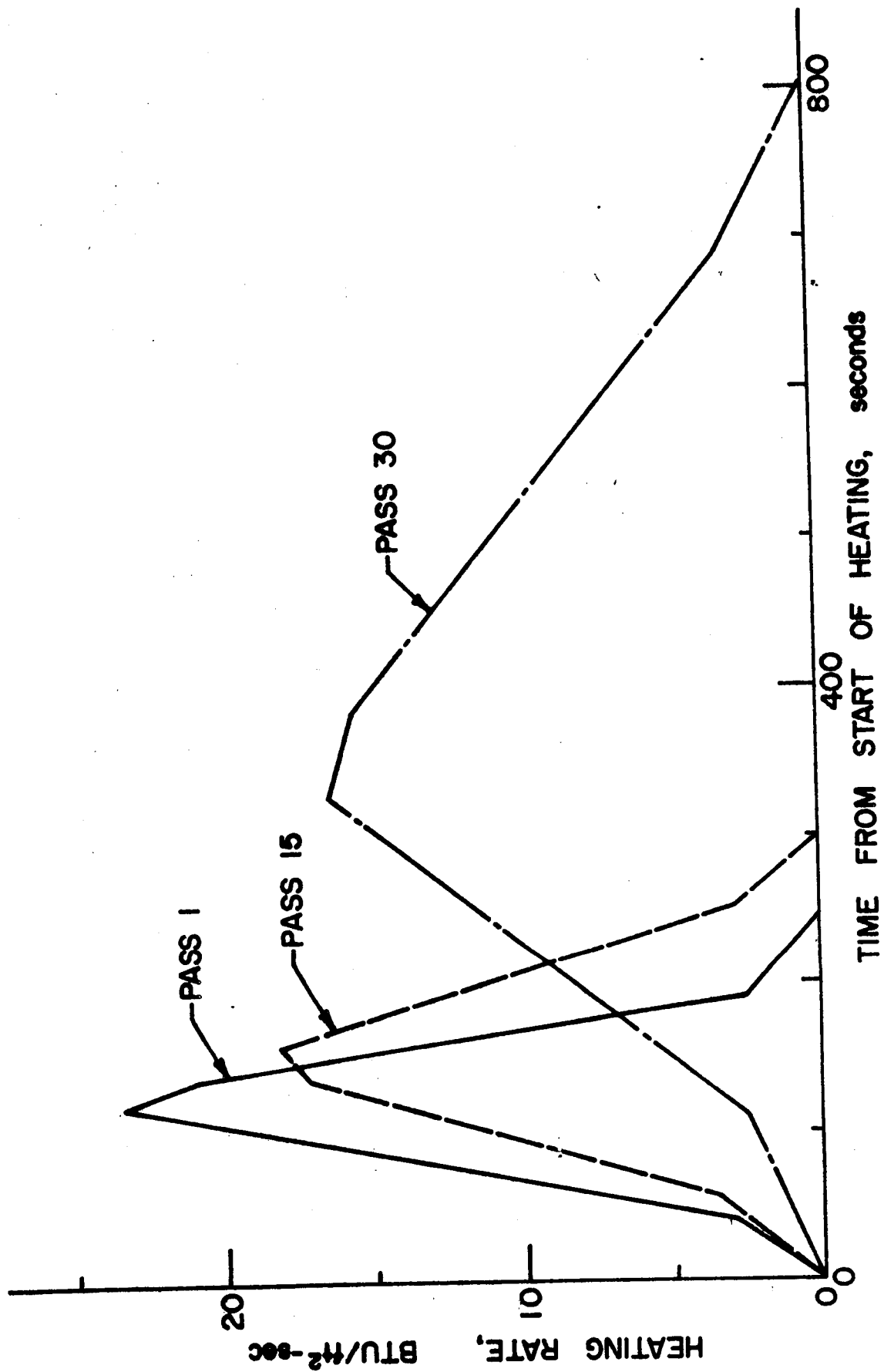
Figure 7 - Modified Heating Rate History for High Drag Configuration - 30 Pass Aerobraking Entry

28
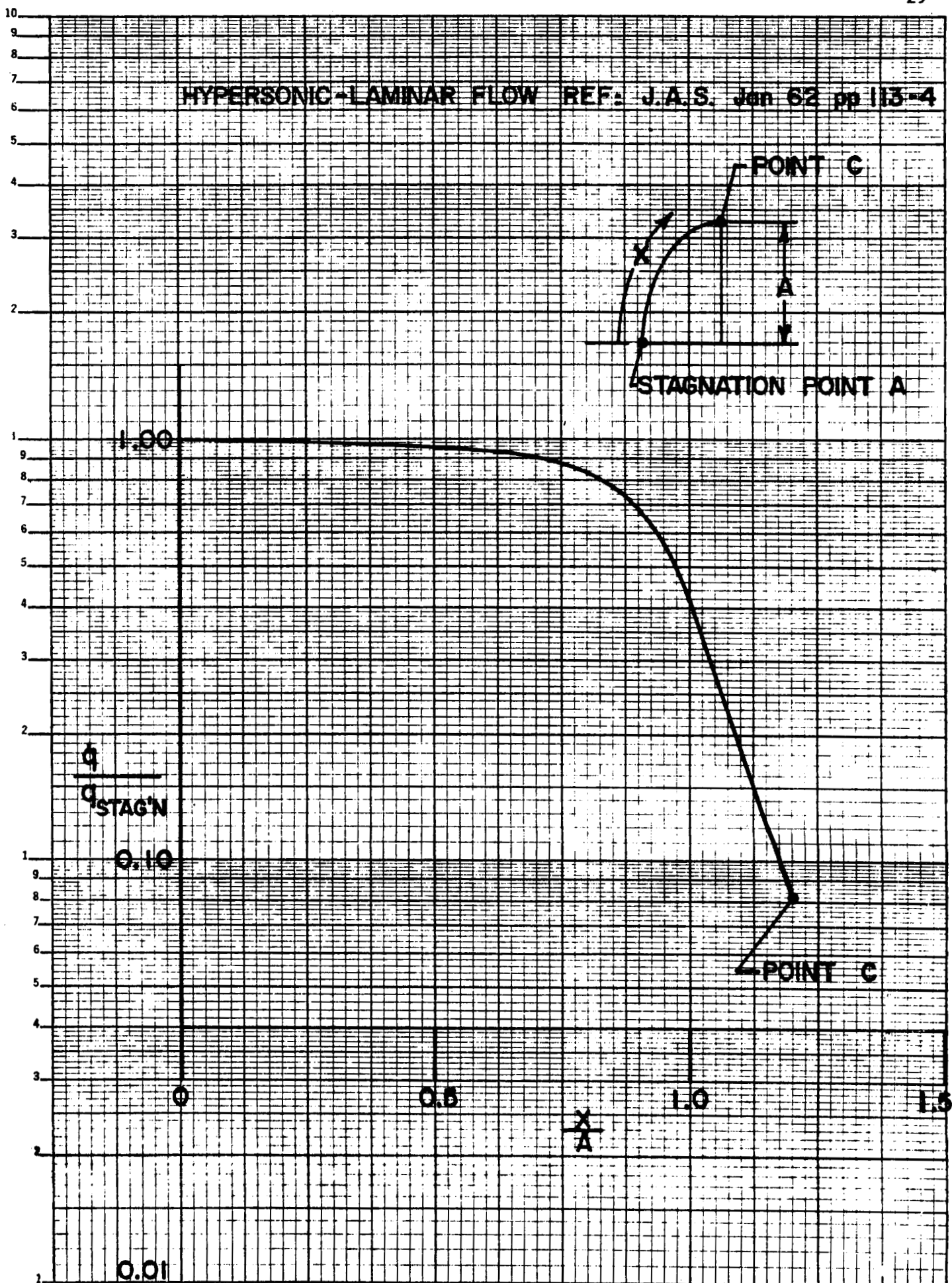
Figure 8 - Heating Rate Distribution for 2:1 Ellipse

Figure 9 - Pressure Distribution for 2:1 Ellipse

The figure is a log-log plot with:
- X-axis: X/D - CAL AFT OF NOSE (from .01 to 10.0)
- Y-axis: LOCAL PRESSURE COEFFICIENT (C_P LOCAL)

Notes listed on the chart:
- NO ABLATION EFFECTS CONSIDERED
- ANGLE OF ATTACK = 0°
- N = NUMBER OF PASSES
- K_n^* IS FUNCTION OF N
- P_L = PRESSURE LOCAL (psf)
- P_L = $C_{P\ LOCAL} \times K_n^*$

N	K_n^*
2	80.
30	8.35

Labels on chart: BOW SHOCK INDUCED PRESSURE FIELD, NOSE CYCL. JCT.
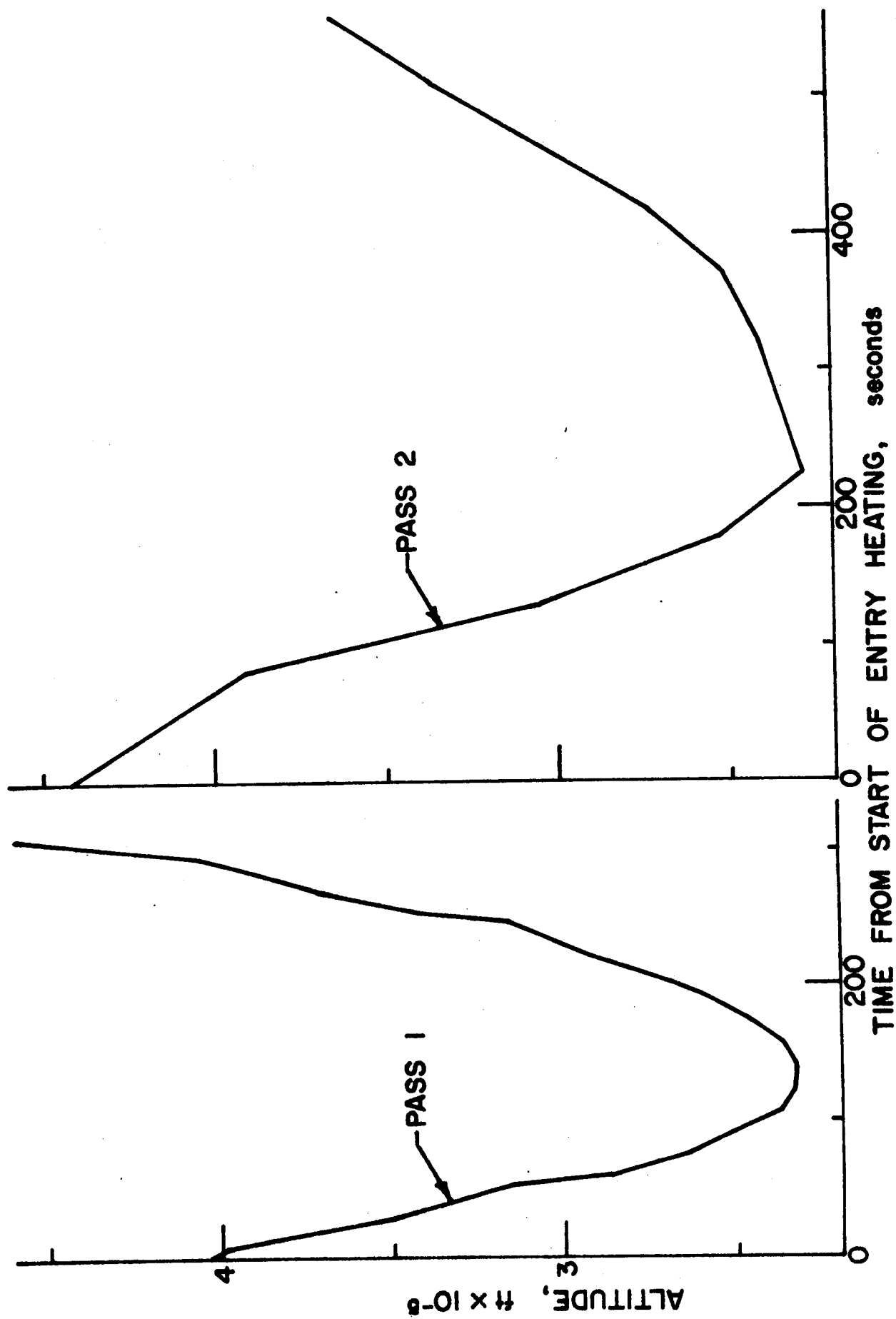
Figure 10 - Altitude-Time History for Low Drag Configuration - 2 Pass Trajectory

31
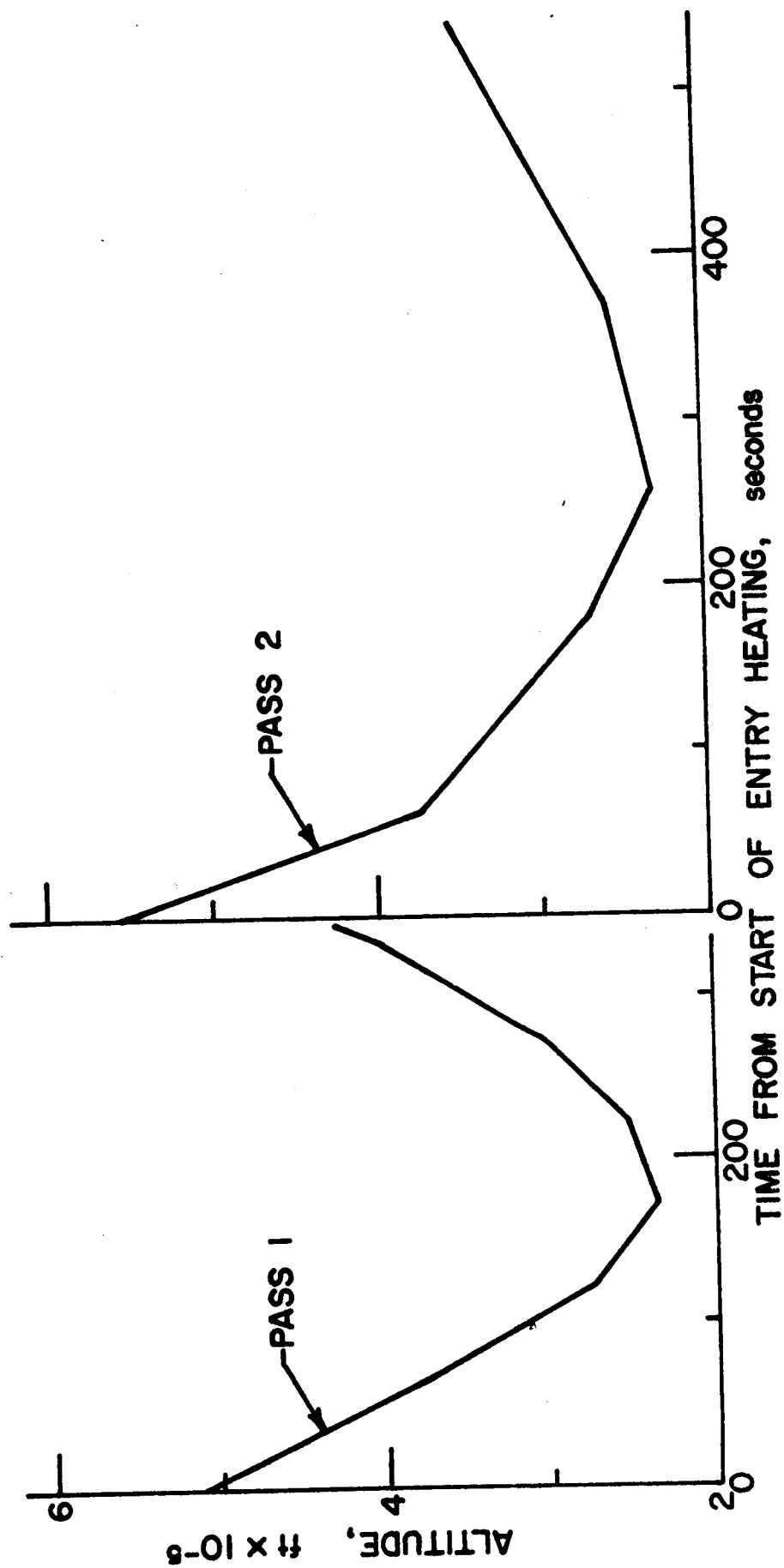
Figure 11 - Altitude-Time History for High Drag Configuration - 2 Pass Trajectory

Figure 12 - Altitude-Time History for High Drag Configuration - 30 Pass Trajectory
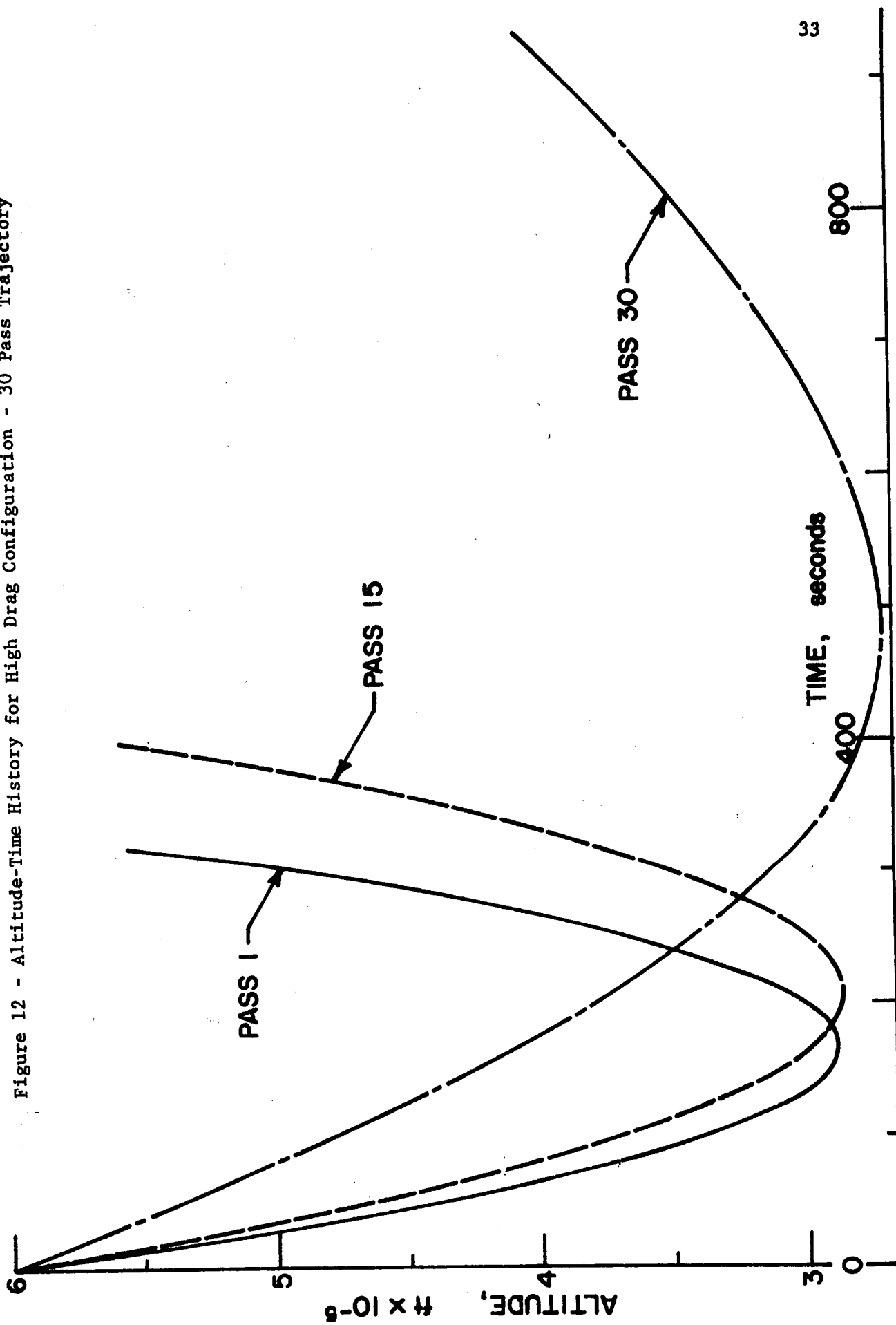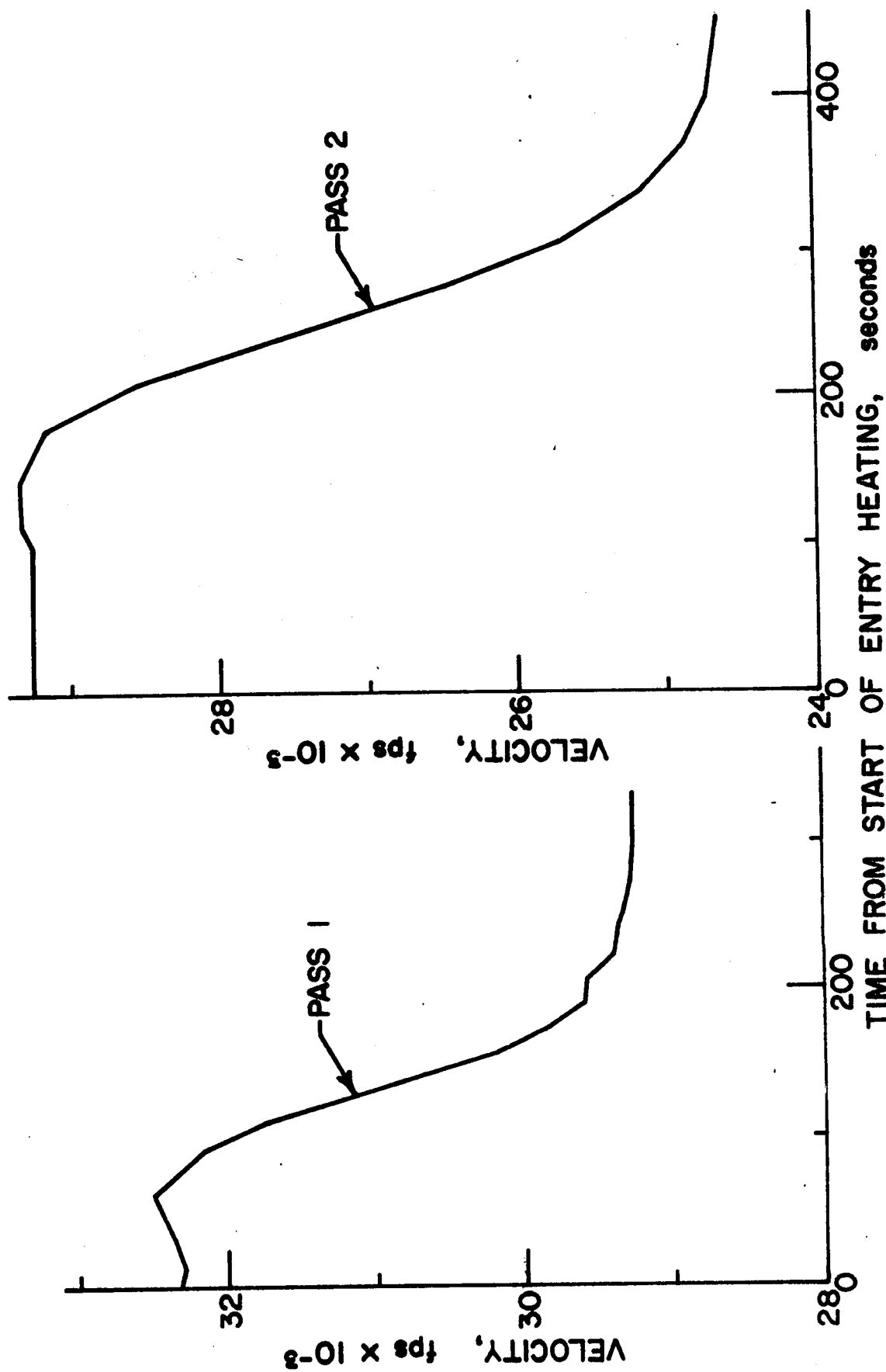
Figure 13 - Velocity-Time History for Low Drag Configuration - 2 Pass Trajectory
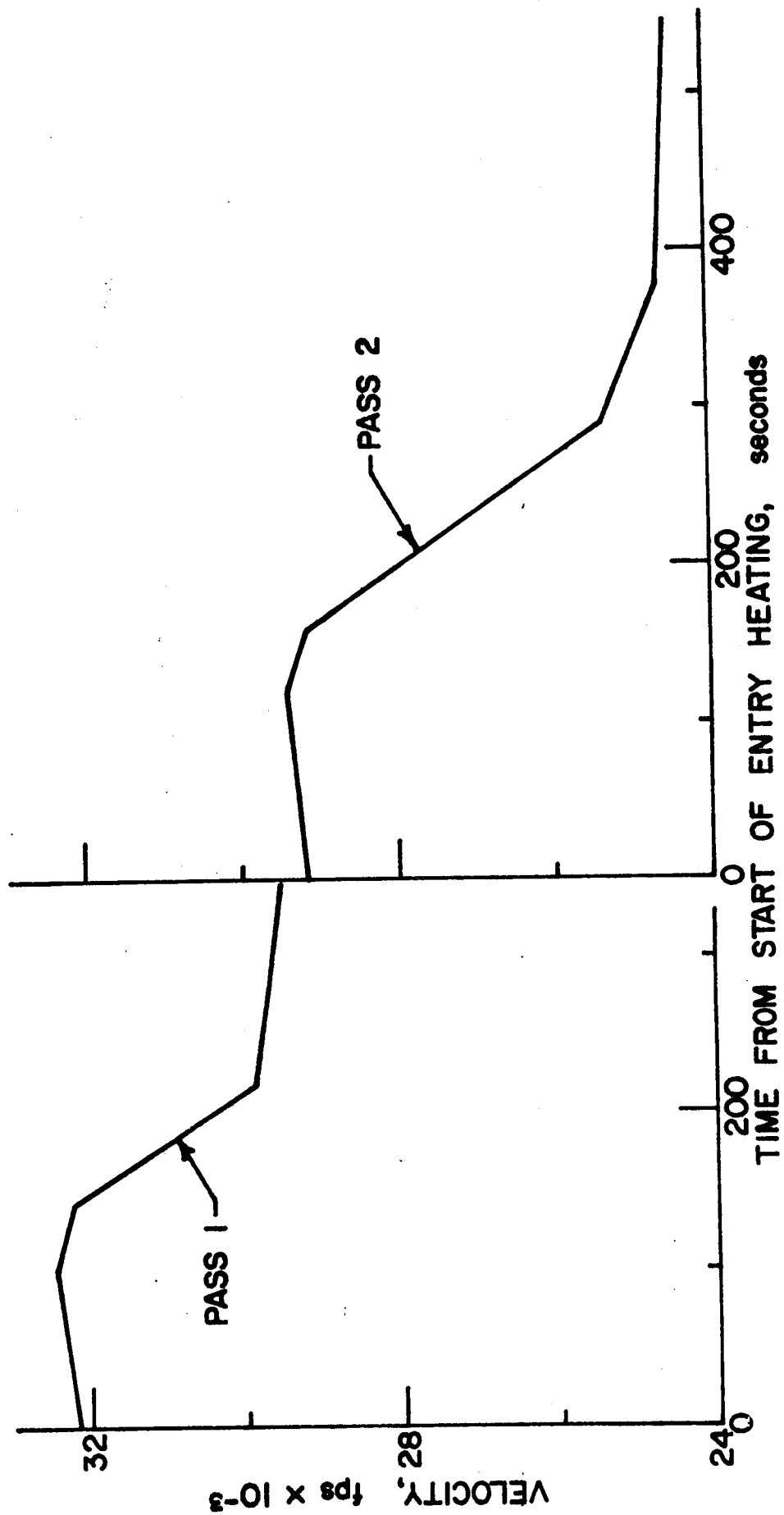
Figure 14 - Velocity-Time History for High Drag Configuration - 2 Pass Trajectory
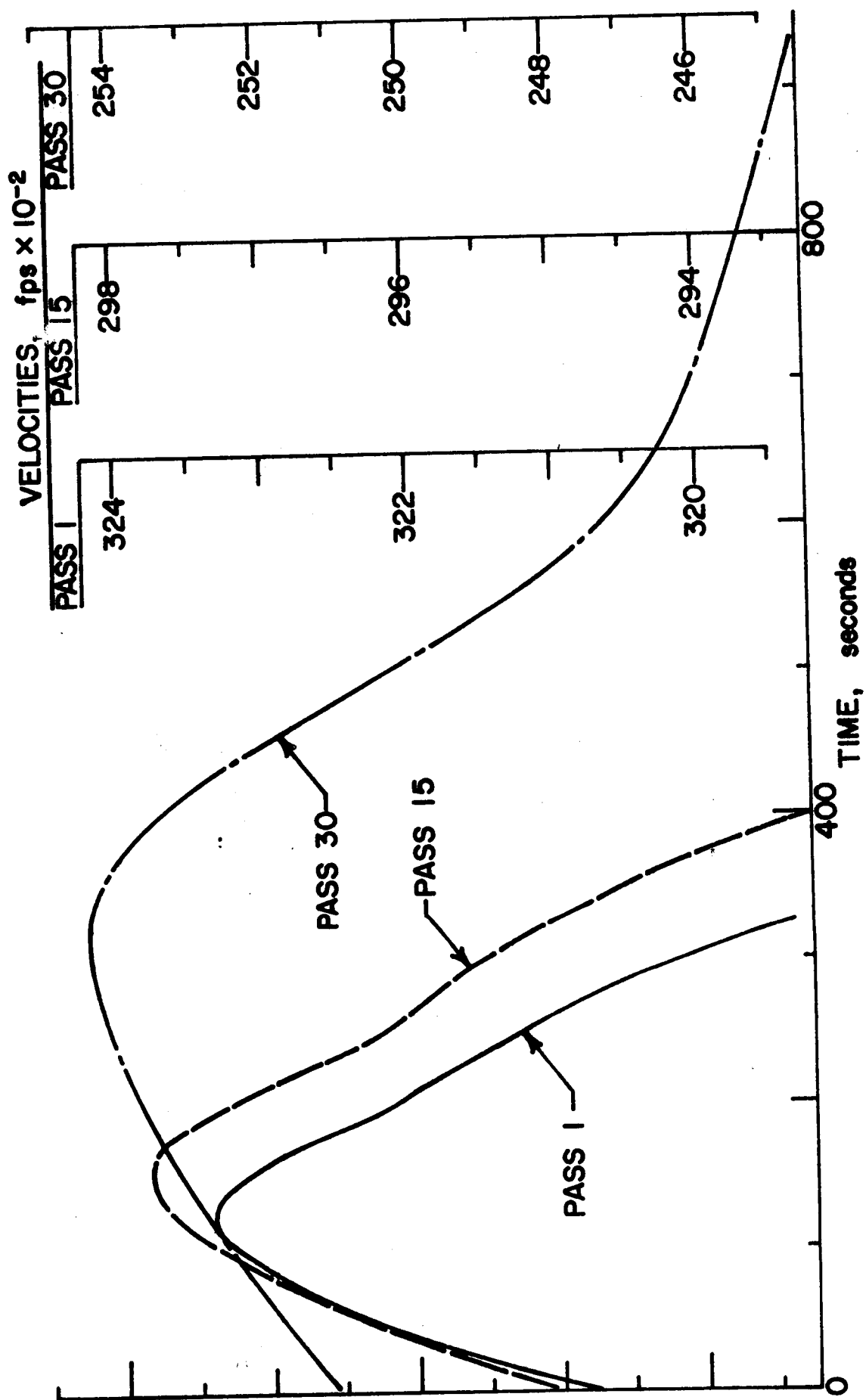
Figure 15 - Velocity-Time History for High Drag Configuration - 30 Pass Trajectory

0.060 Aluminum Skin

2 : 1 Ellipse
14 ft Dia

7.25 ft

1.5 x 6 Channel

3 x 3
I Beam

2 x 2
Channel
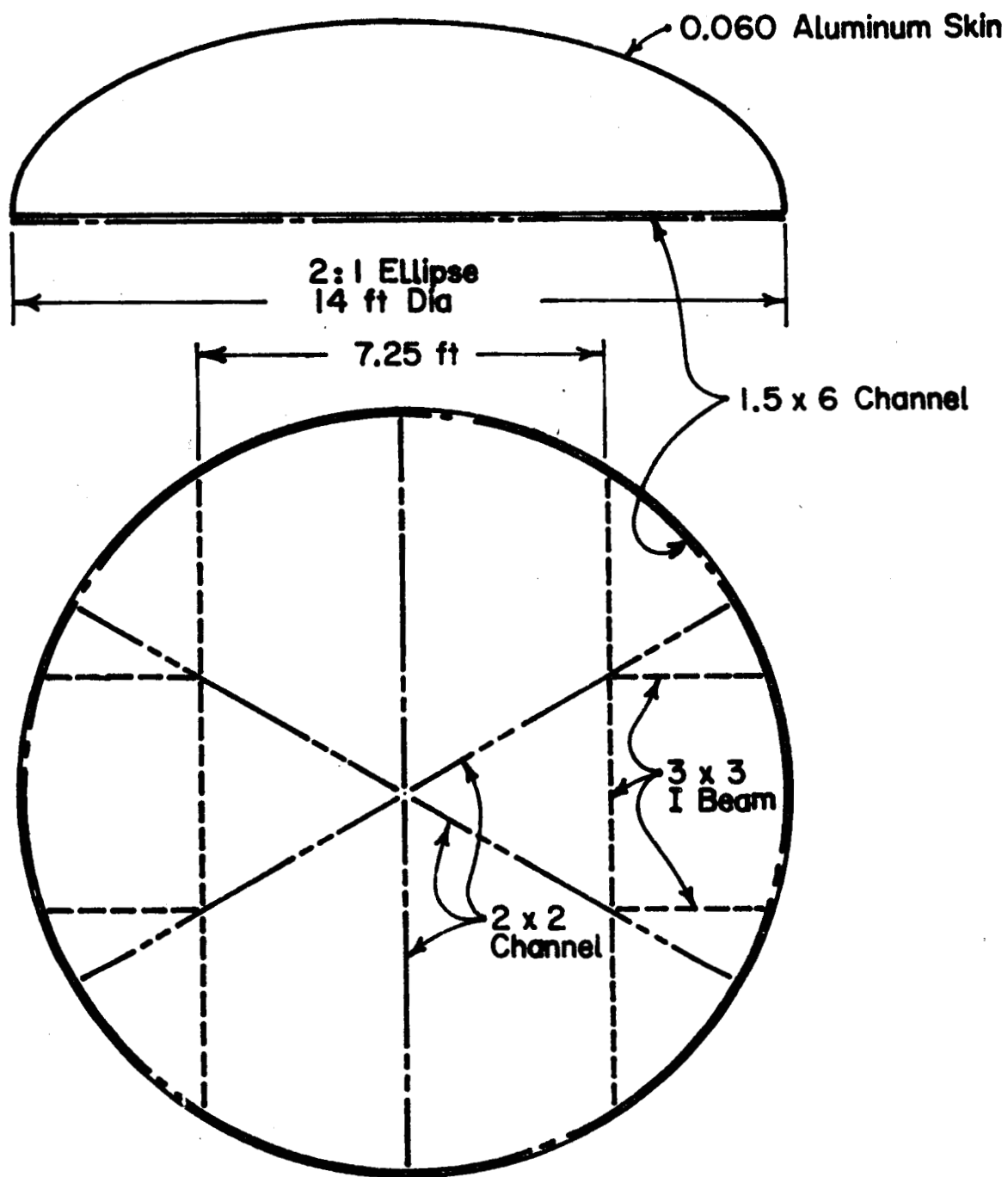
**ALUMINUM DOME STRUCTURE FOR
ABLATIVE SHIELDING**

Figure 16 - Aluminum Dome Structure for Ablative Shielding
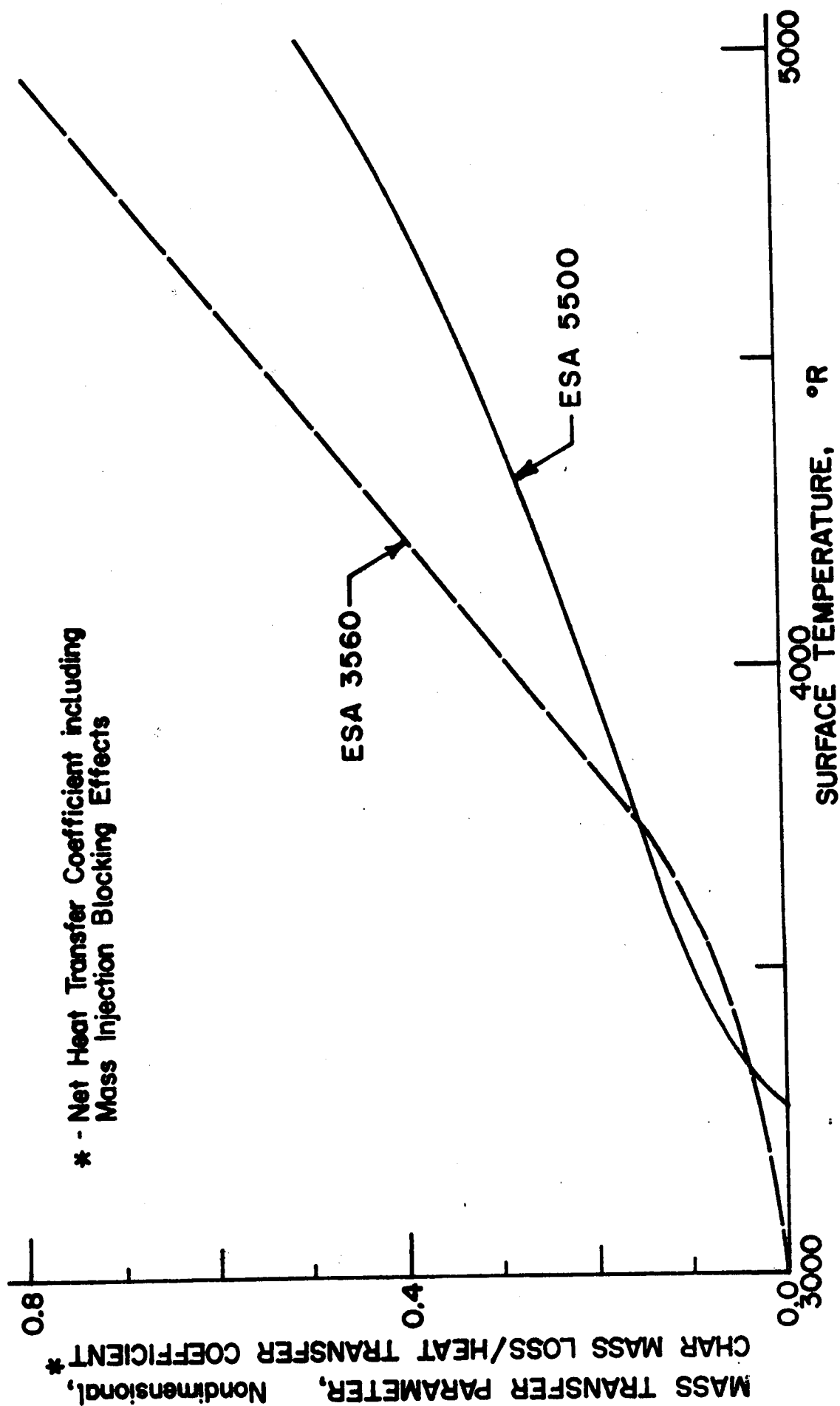
Figure 17 - Char Mass Loss for Silicone Ablators ESA 5500 and ESA 3560

38
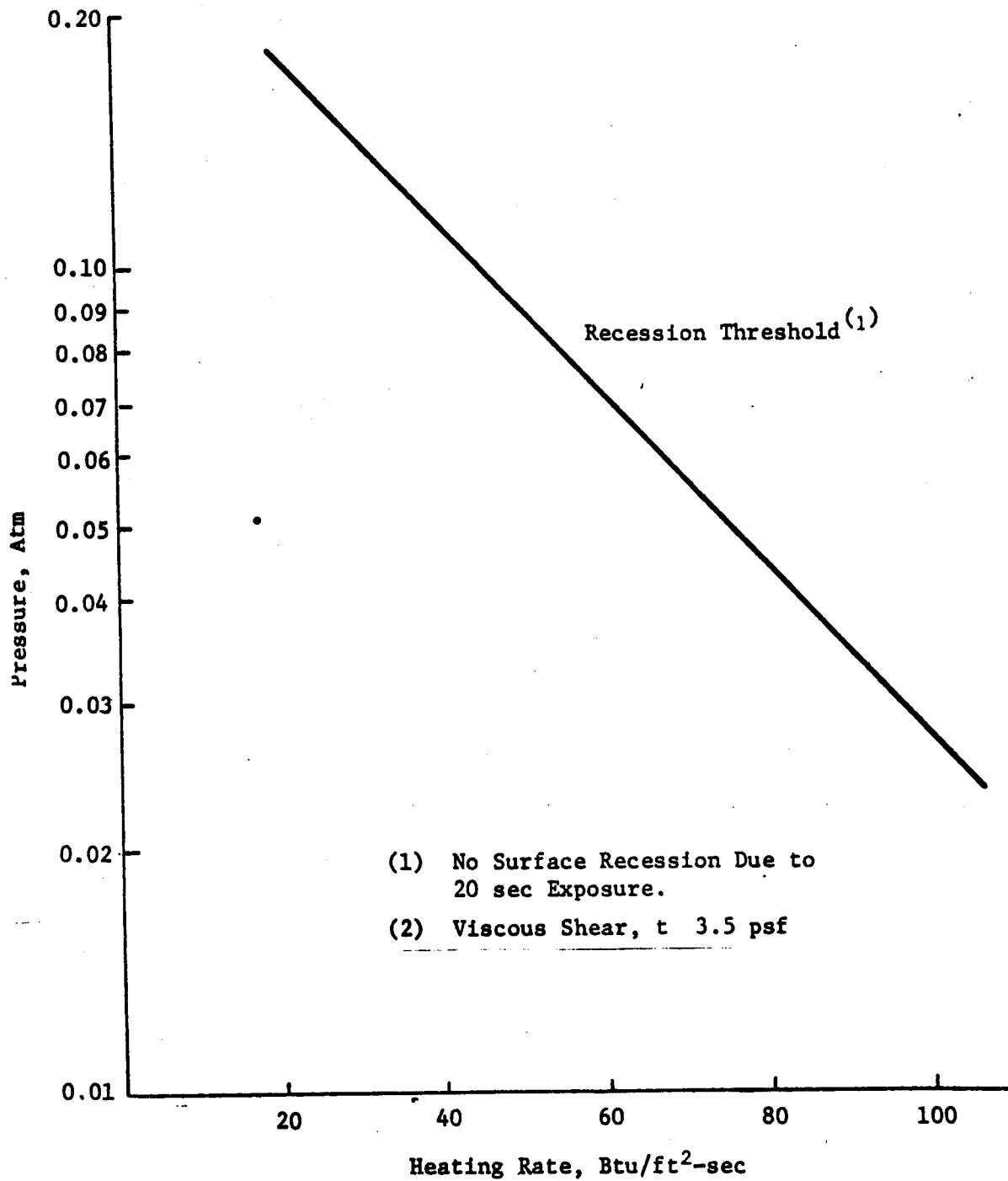
Figure 18 - Recession Threshold for SLA-561
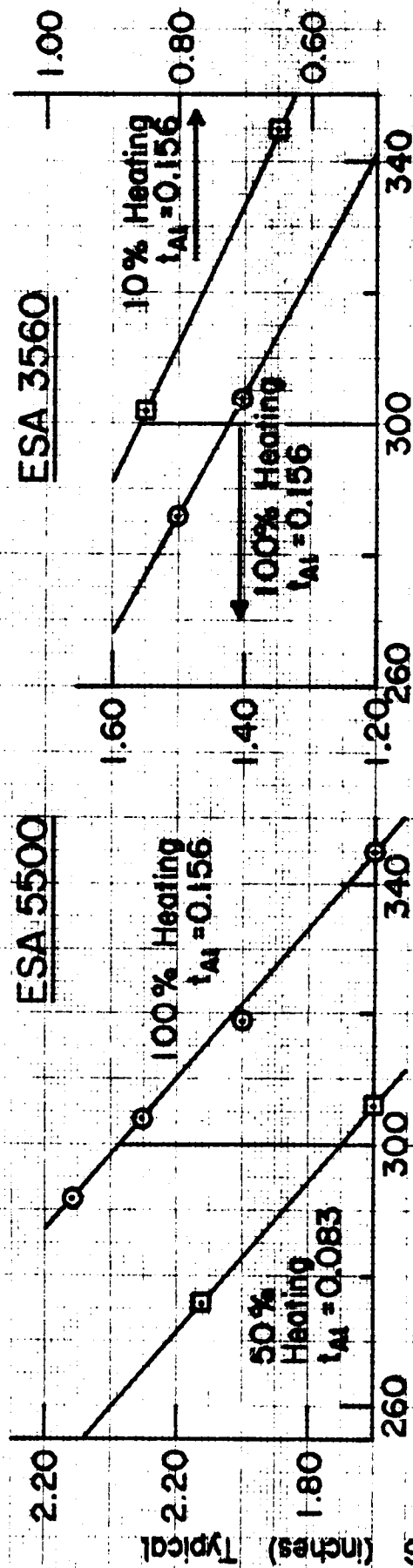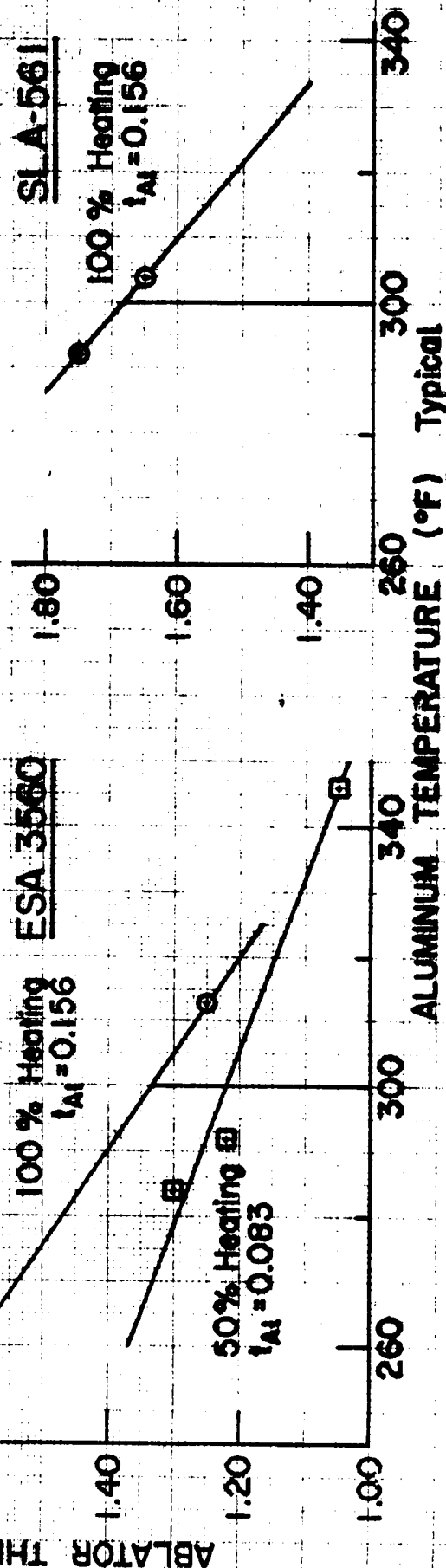
Figure 19 - Ablator Thickness Requirements for 300°F Aluminum Temperature - Two Pass Entry
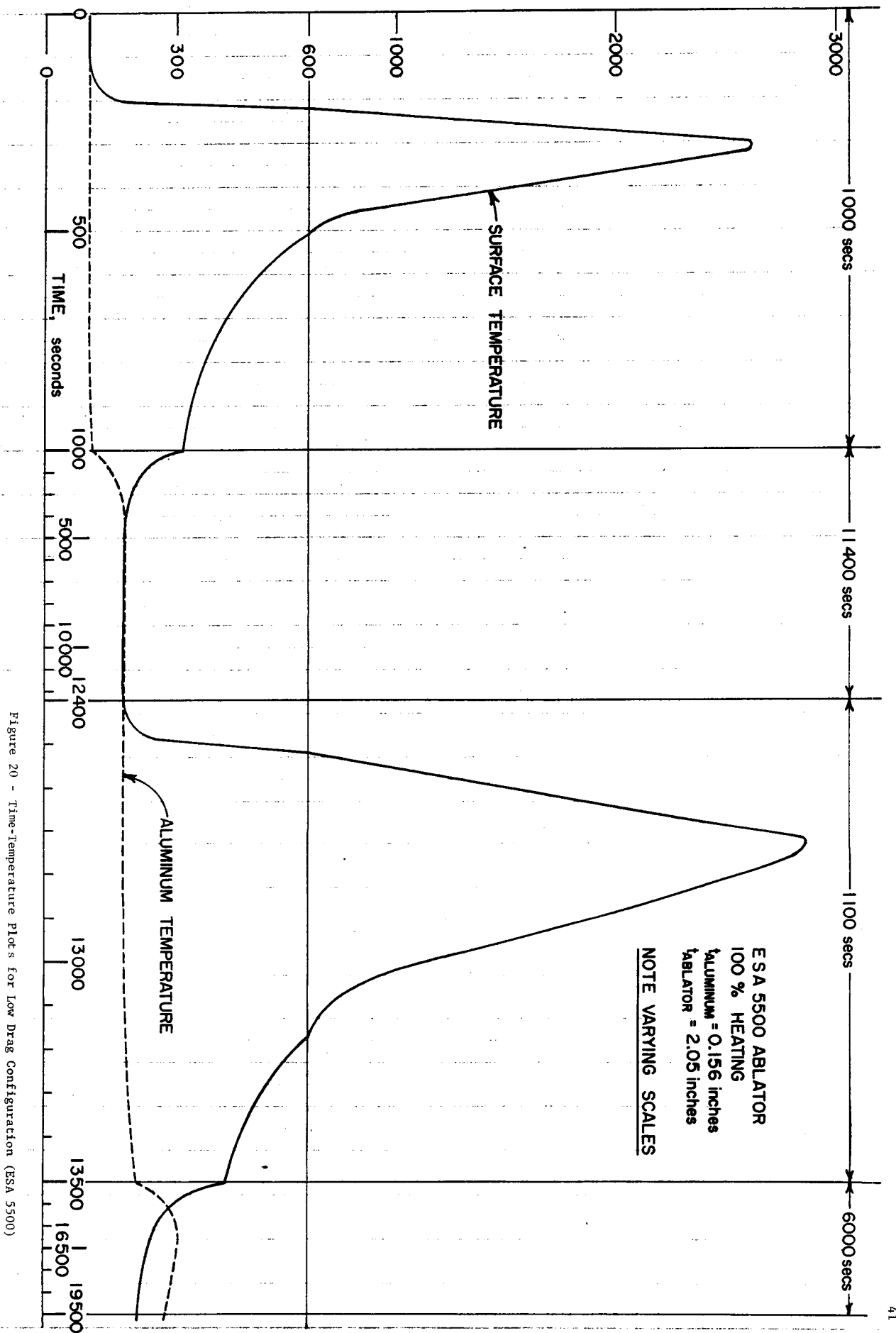
Figure 20 - Time-Temperature Plots for Low Drag Configuration (ESA 5500)

SURFACE TEMPERATURE

ALUMINUM TEMPERATURE

TIME, seconds

E S A 5500 ABLATOR
100 % HEATING
$t_{ALUMINUM}$ = 0.156 inches
$t_{ABLATOR}$ = 2.05 inches

NOTE VARYING SCALES

3000

2000

1000

600

300

0

1000 secs

11400 secs

1100 secs

6000 secs

0   500   1000   5000   10000   12400   13000   13500   16500 19500

41
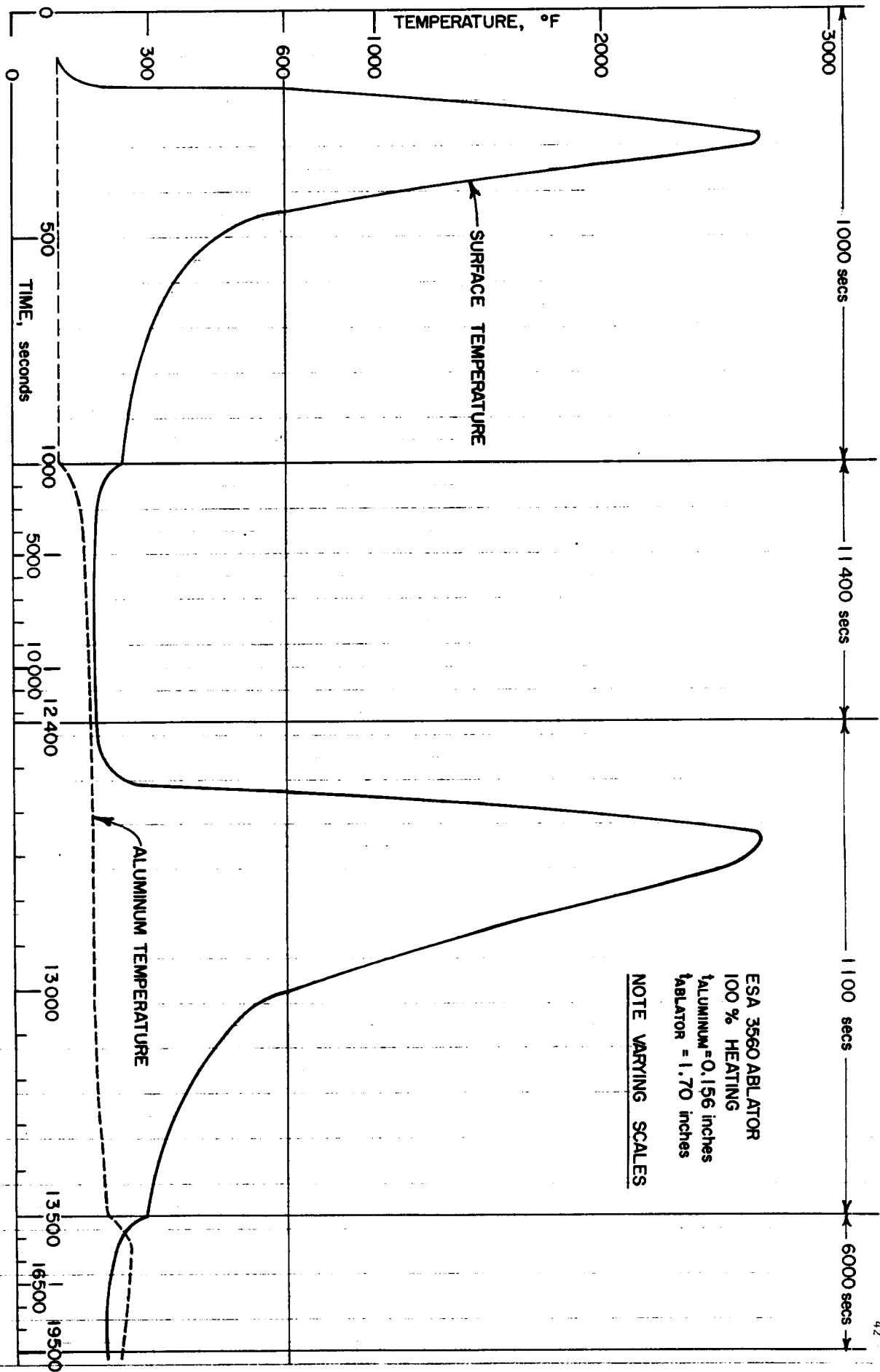
Figure 21 - Time-Temperature Plots for High Drag Configuration

TEMPERATURE, °F

SURFACE TEMPERATURE

ALUMINUM TEMPERATURE

ESA 3560 ABLATOR
100 % HEATING
$t_{ALUMINUM} = 0.156$ inches
$t_{ABLATOR} = 1.70$ inches

NOTE VARYING SCALES

TIME, seconds

1000 secs

11400 secs

1100 secs

6000 secs

42

Figure 21 - Continued

SLA 561 ABLATOR
100 % HEATING
$t_{ALUMINUM}$ = 0.083 inches
$t_{ABLATOR}$ = 1.80 inches

NOTE VARYING SCALES

43
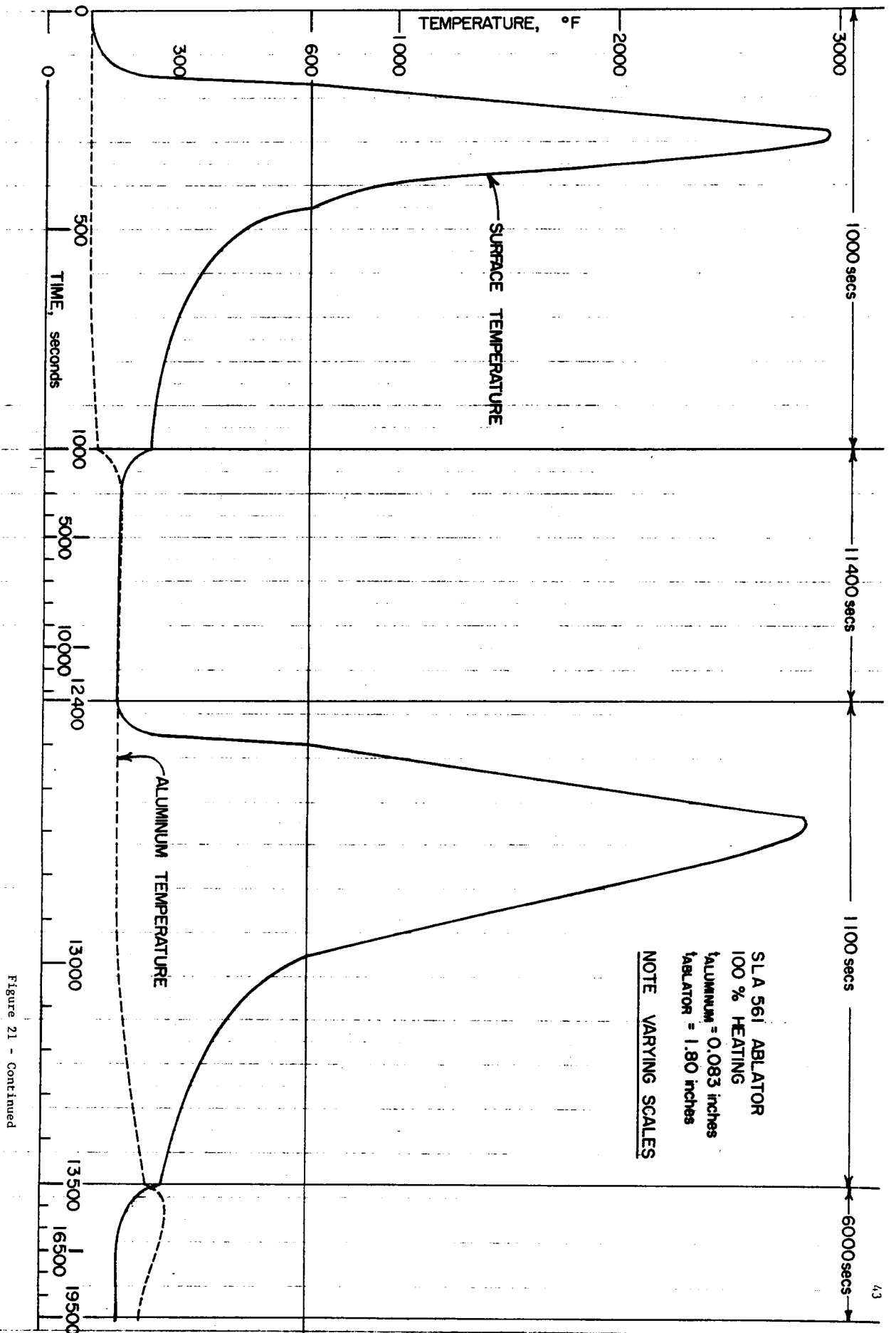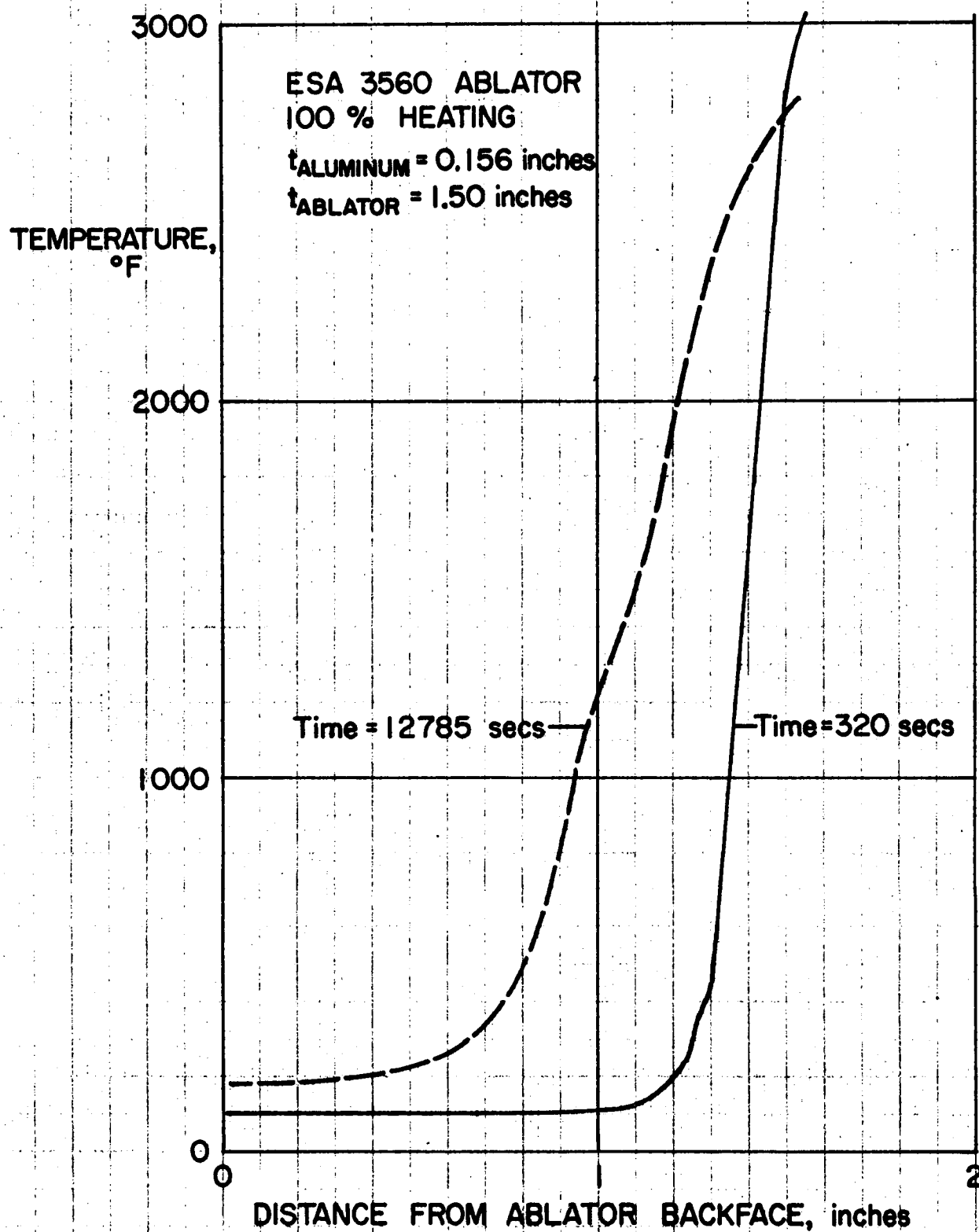
Figure 22 - Temperature Distribution through Ablator During First and Second Heating Pulse
Low Drag Configuration
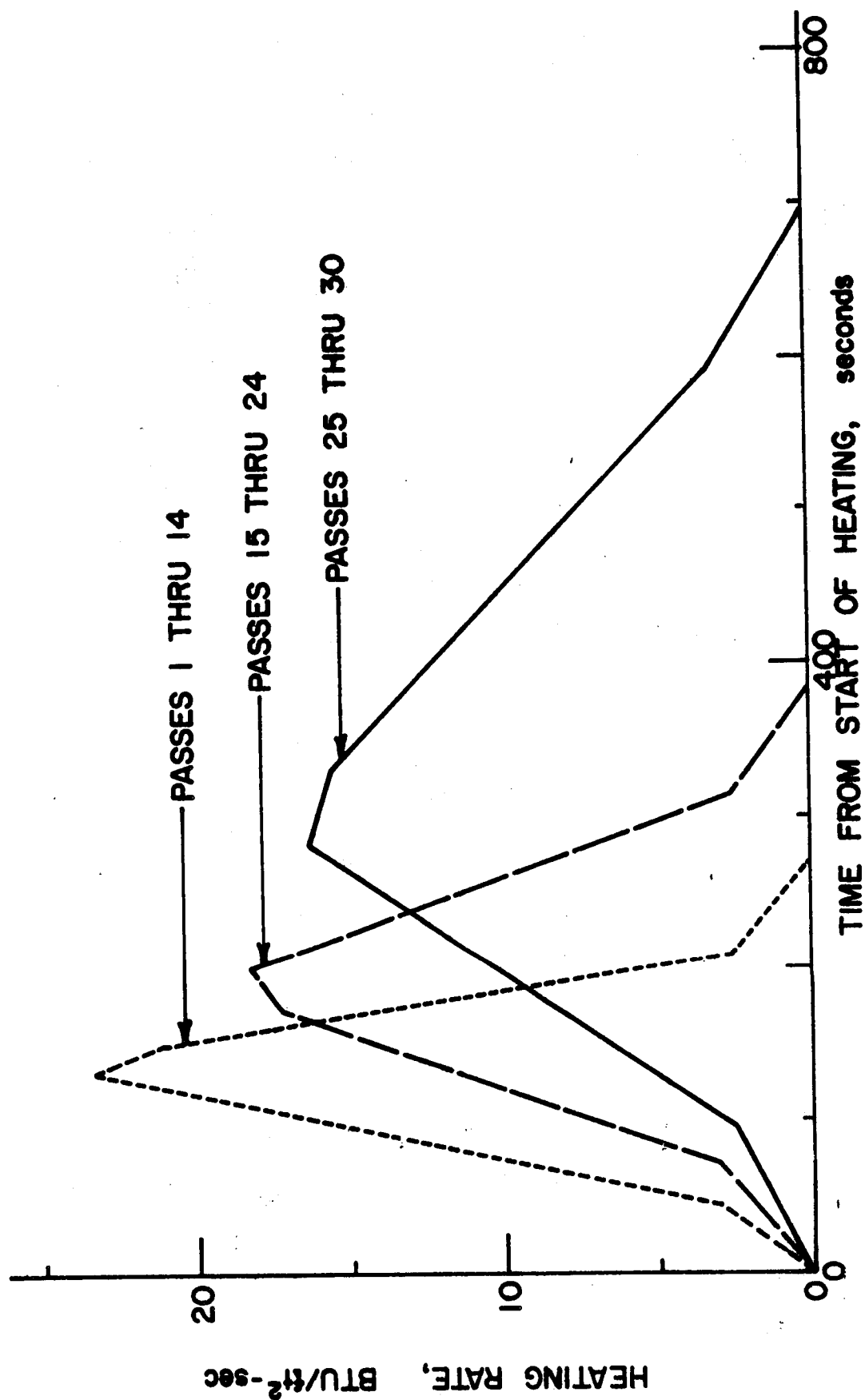
Figure 23 - Shape of Average Heat Pulses for 30 Pass Entry, High Drag Configuration
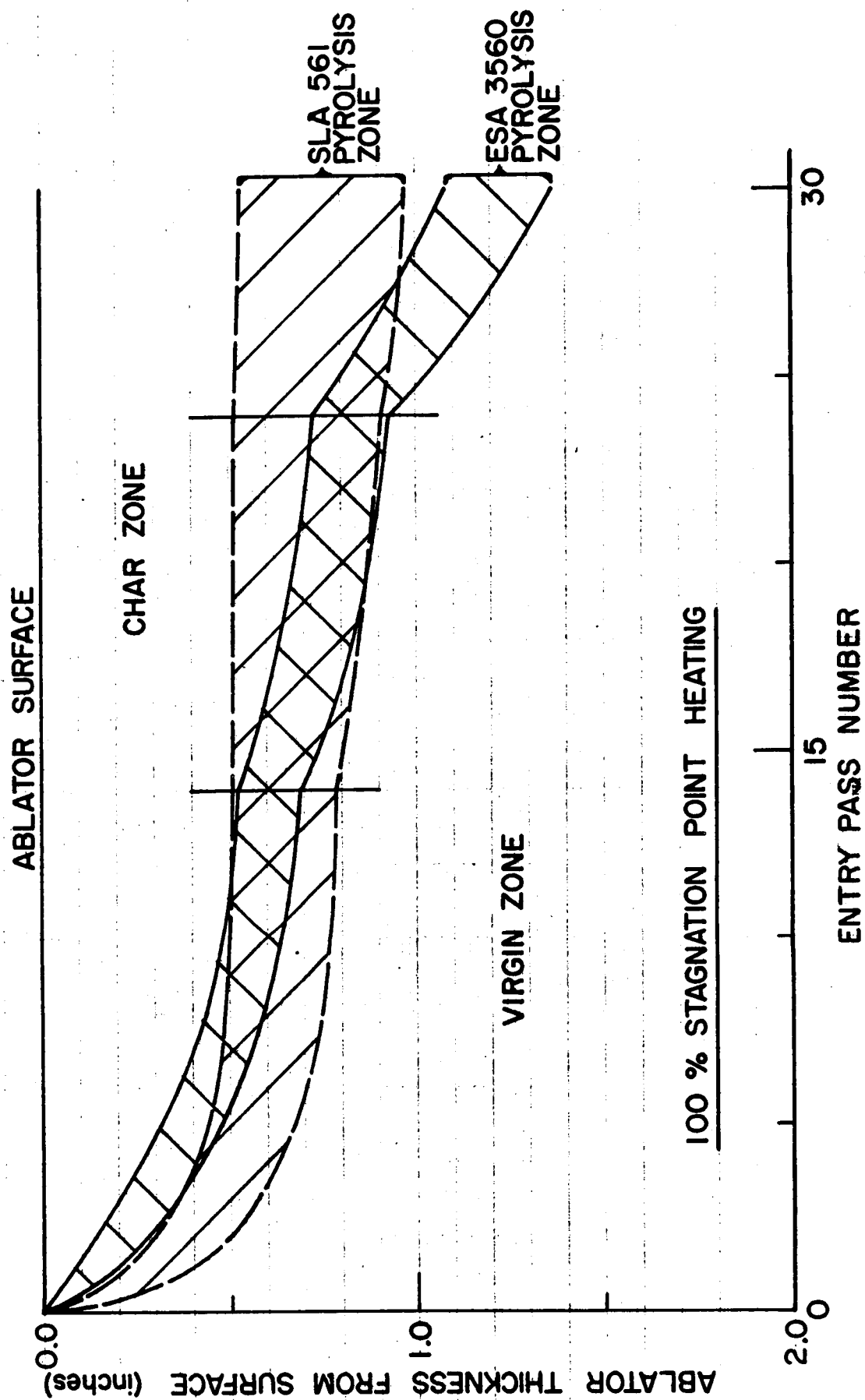
Figure 24 - Progression of Char Formation and Pyrolysis During Thirty Pass Entry for High Drag Configuration

ABLATOR SURFACE

CHAR ZONE

PYROLYSIS
ZONES:
SLA 561
ESA 3560

VIRGIN ZONE

50 % STAGNATION POINT HEATING

ENTRY PASS NUMBER

ABLATOR THICKNESS FROM SURFACE (inches)
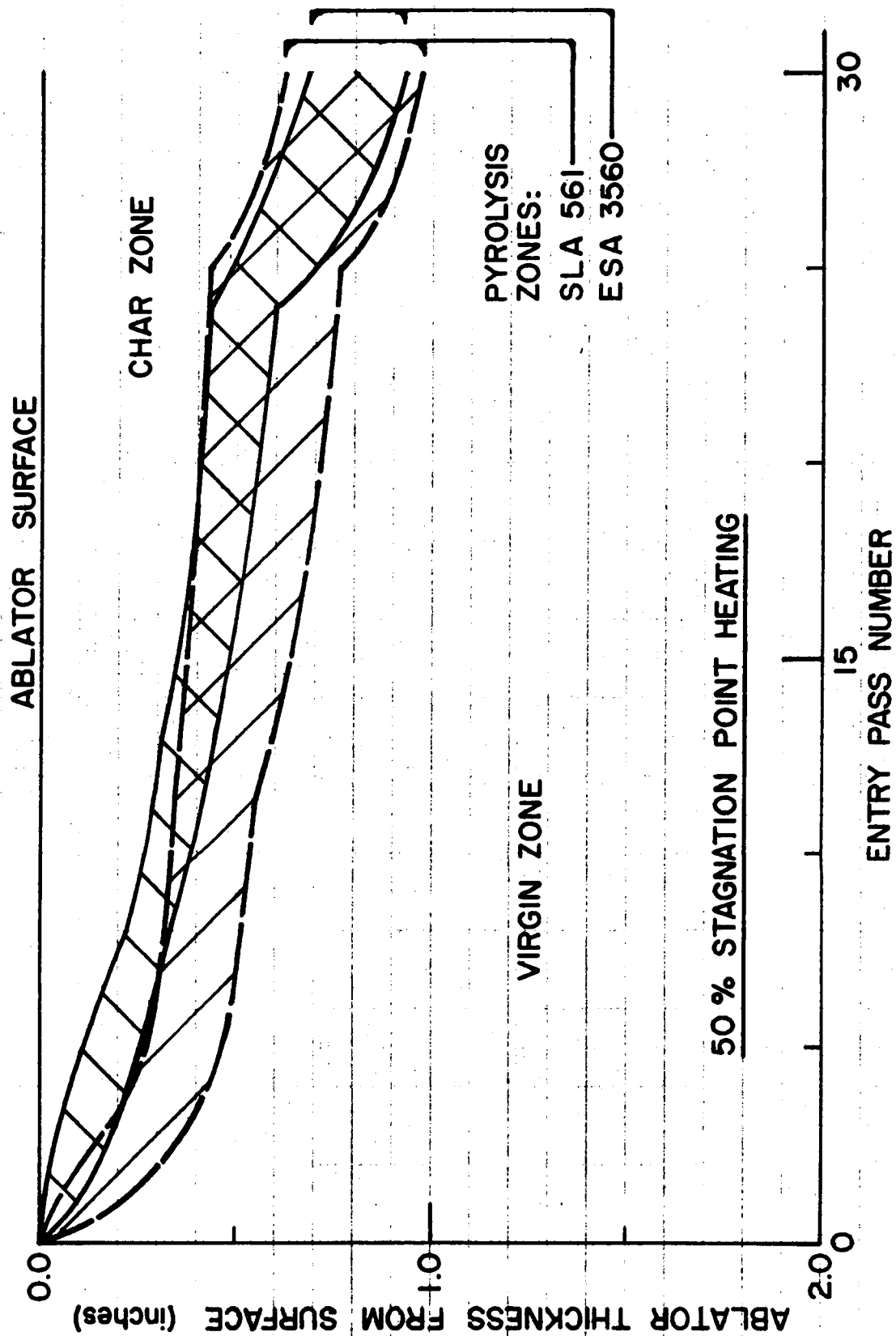
Figure 24 Continued
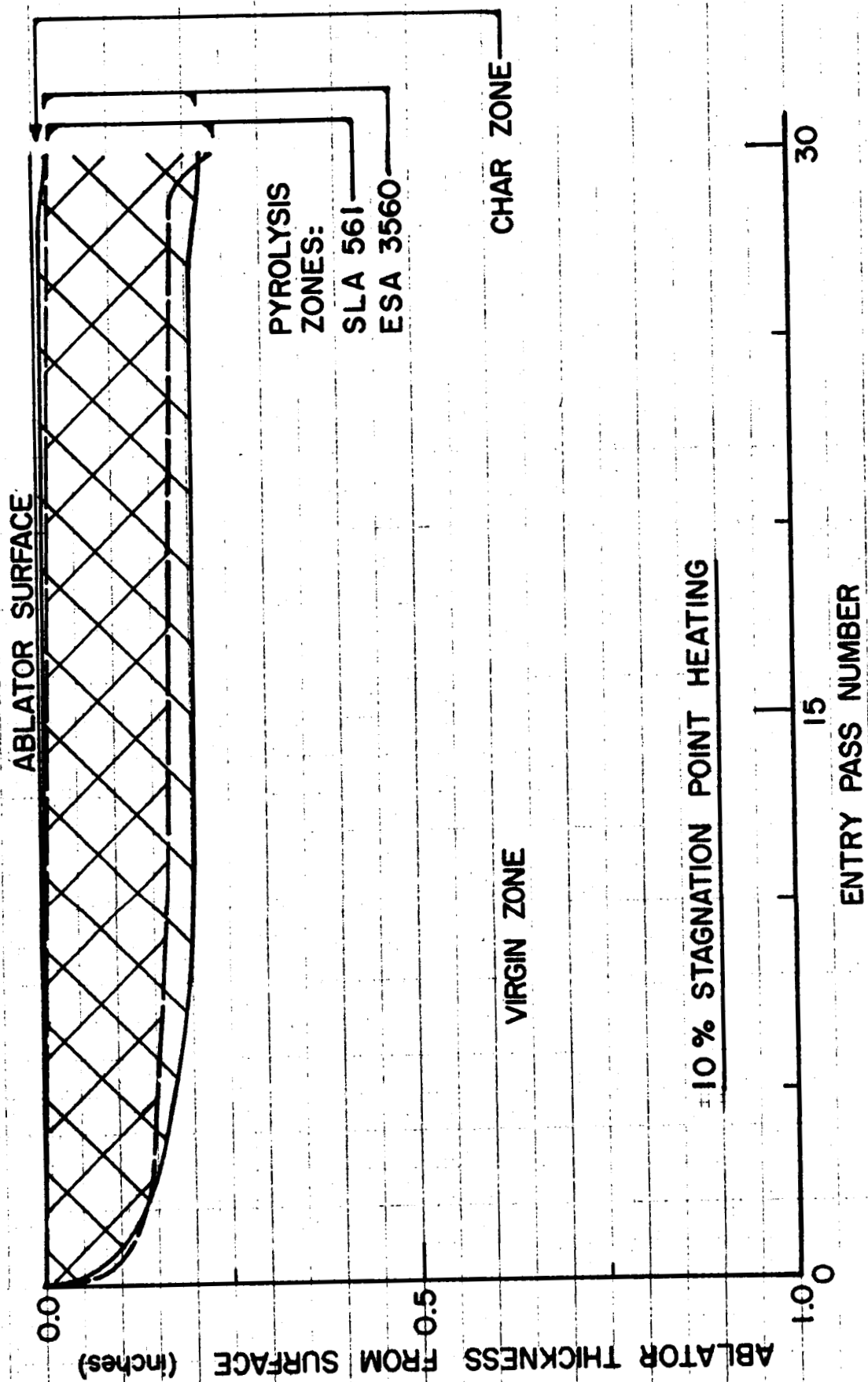
Figure 24 Continued
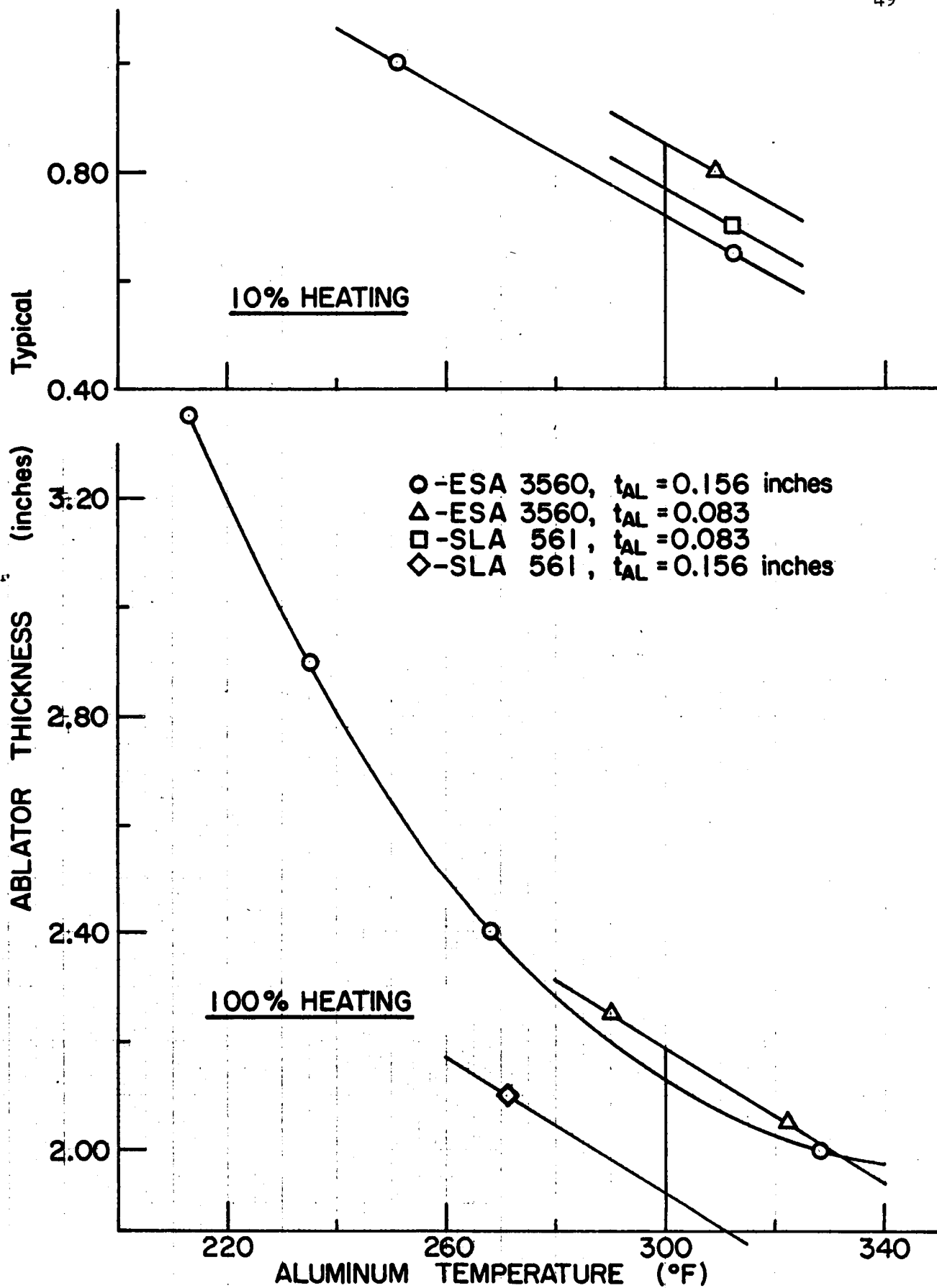
Figure 25 - Ablator Thickness Requirements for 300°F Aluminum Temperature - Thirty Pass Entry
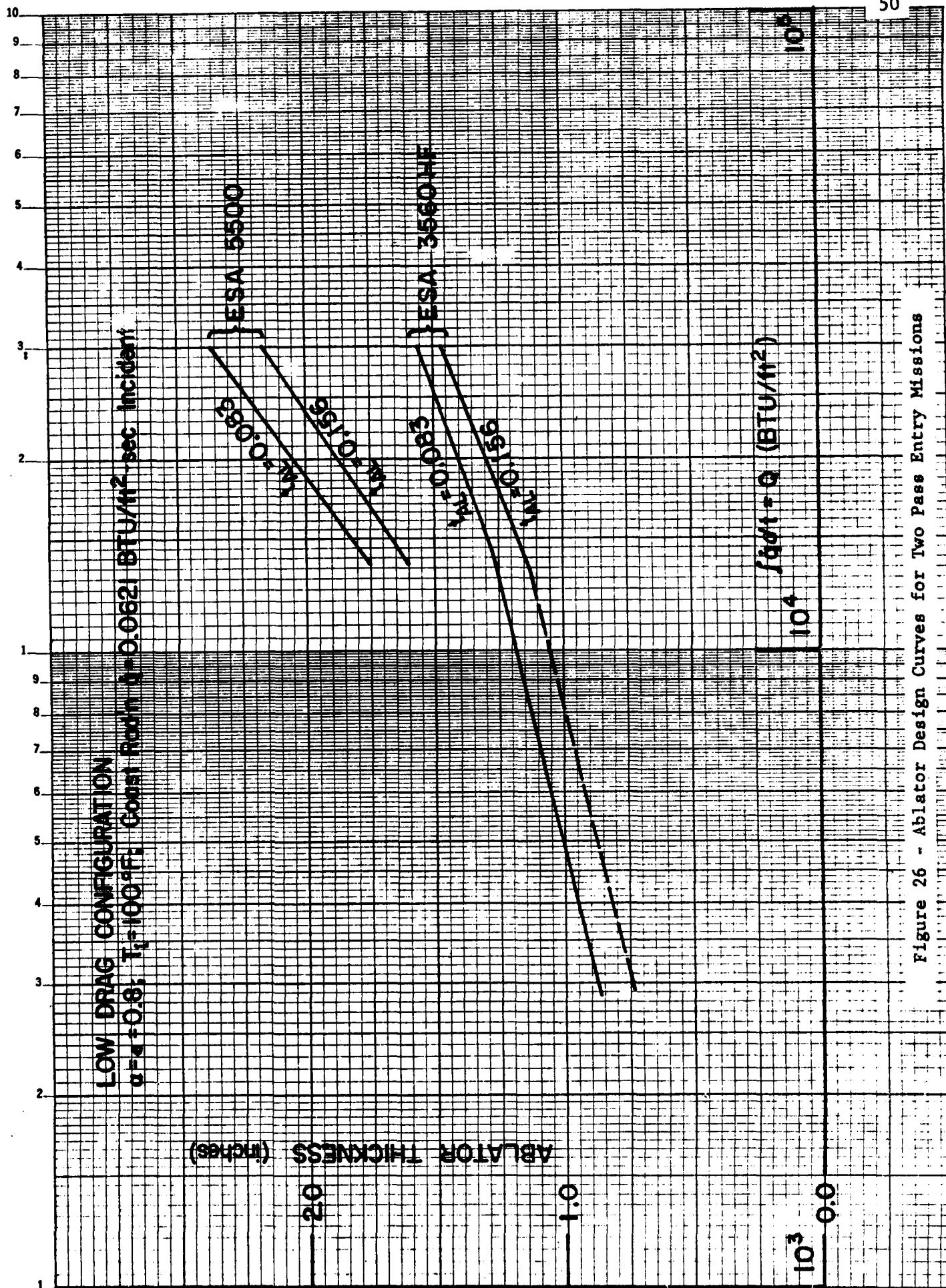
Figure 26 - Ablator Design Curves for Two Pass Entry Missions
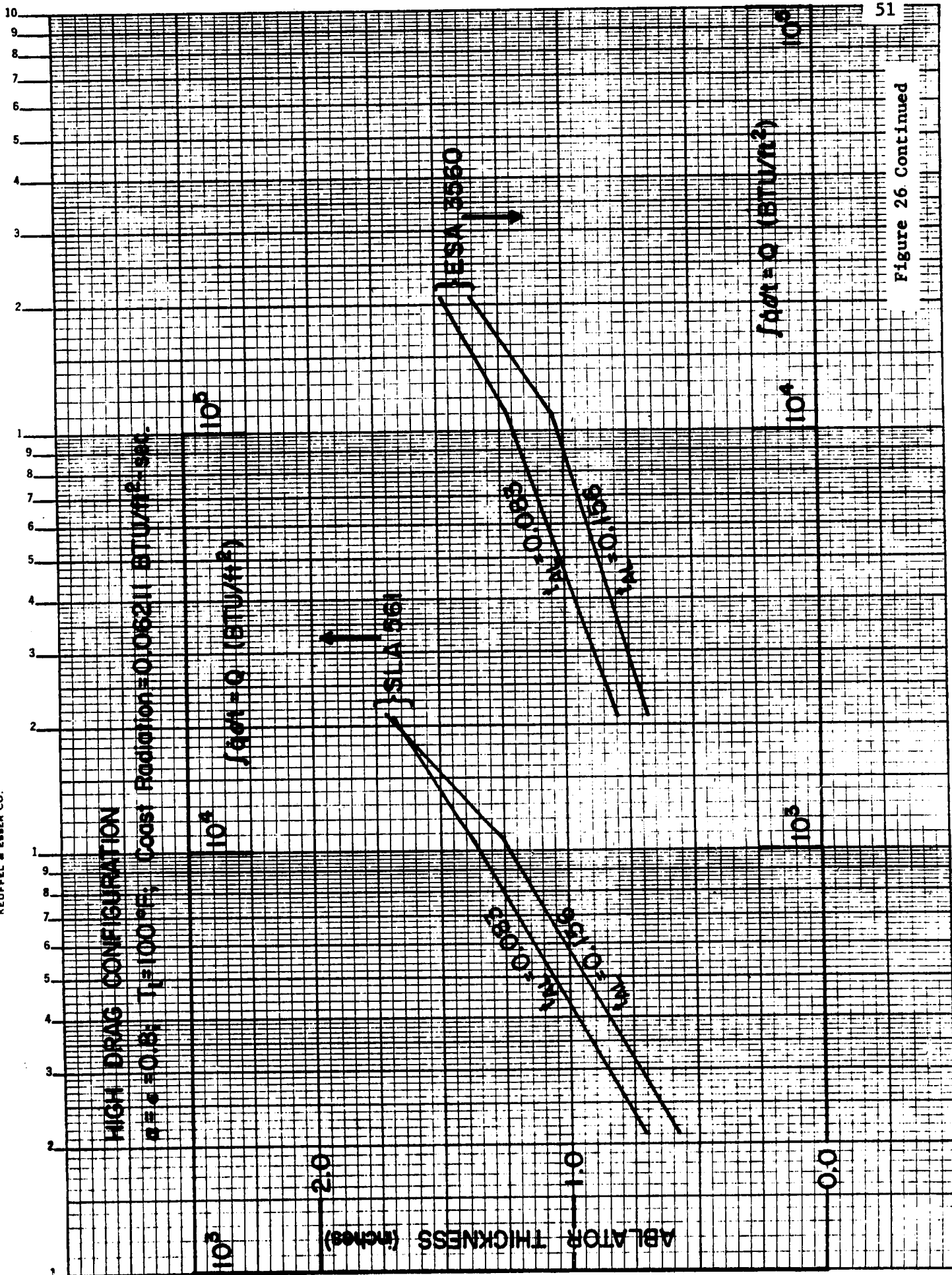
Figure 26 Continued
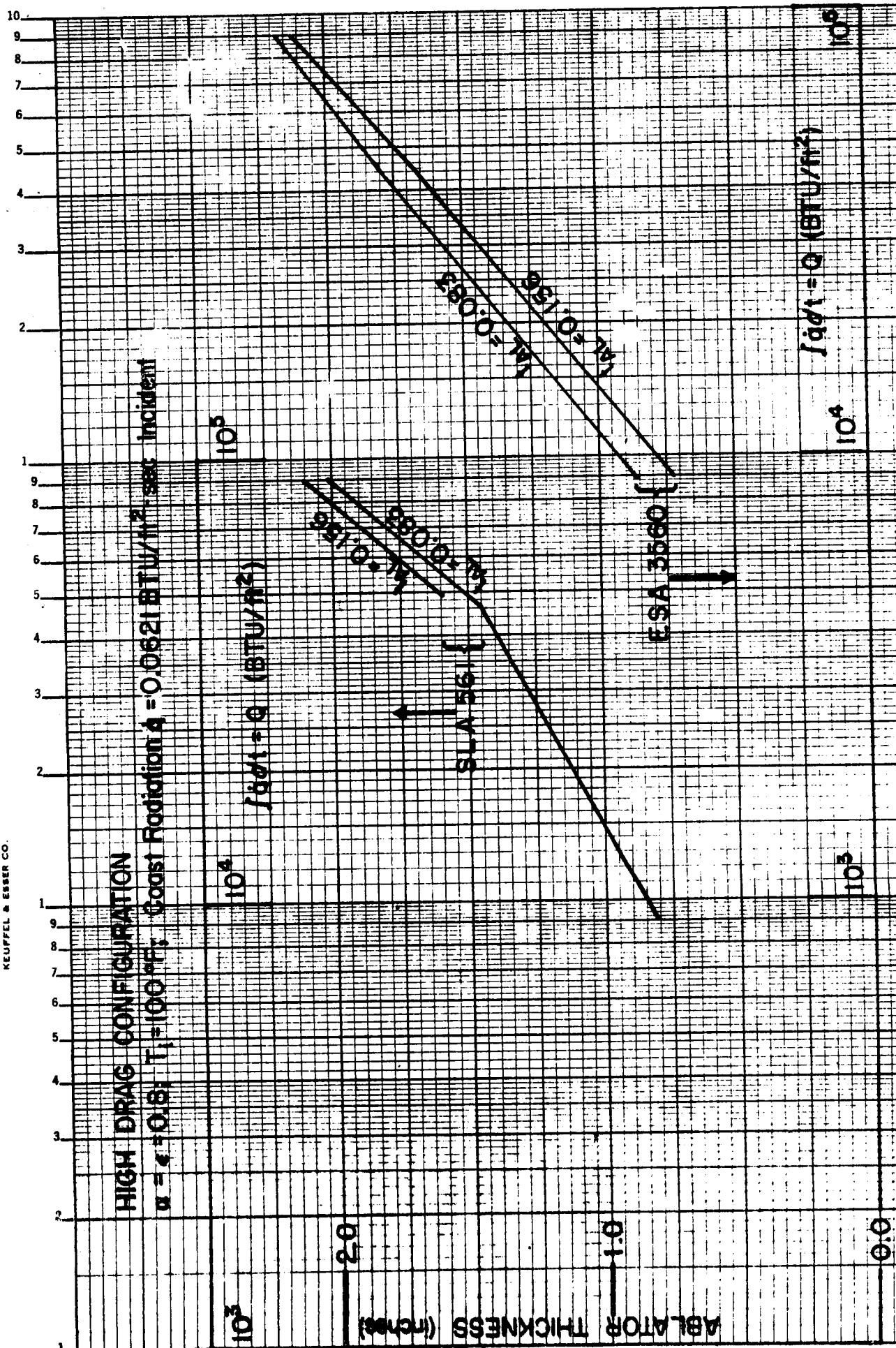
Figure 27 - Ablator Design Curves for Thirty Pass Entry Missions
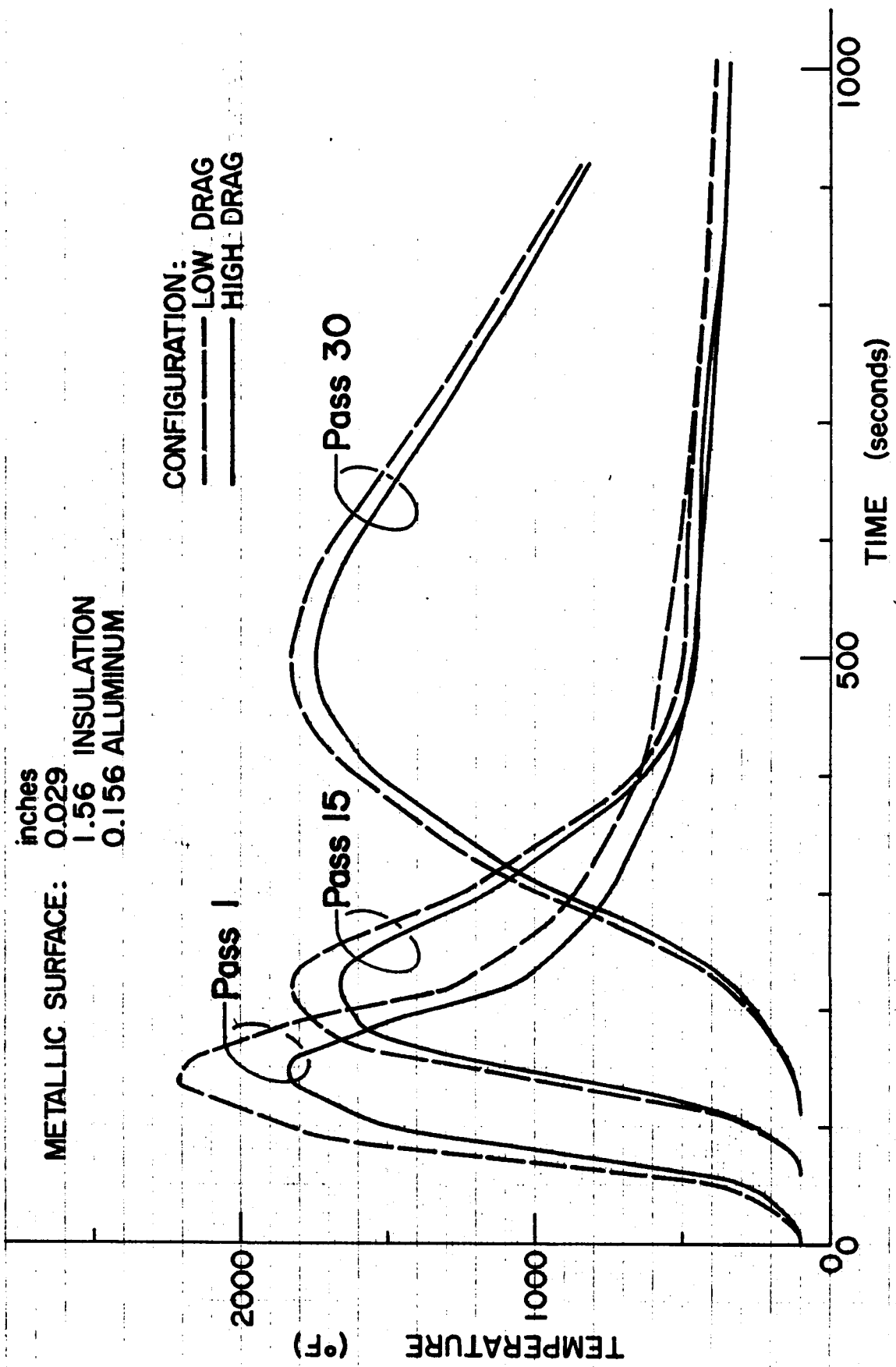
Figure 28 – Temperature Histories for Metallic Heat Shields at Stagnation Point
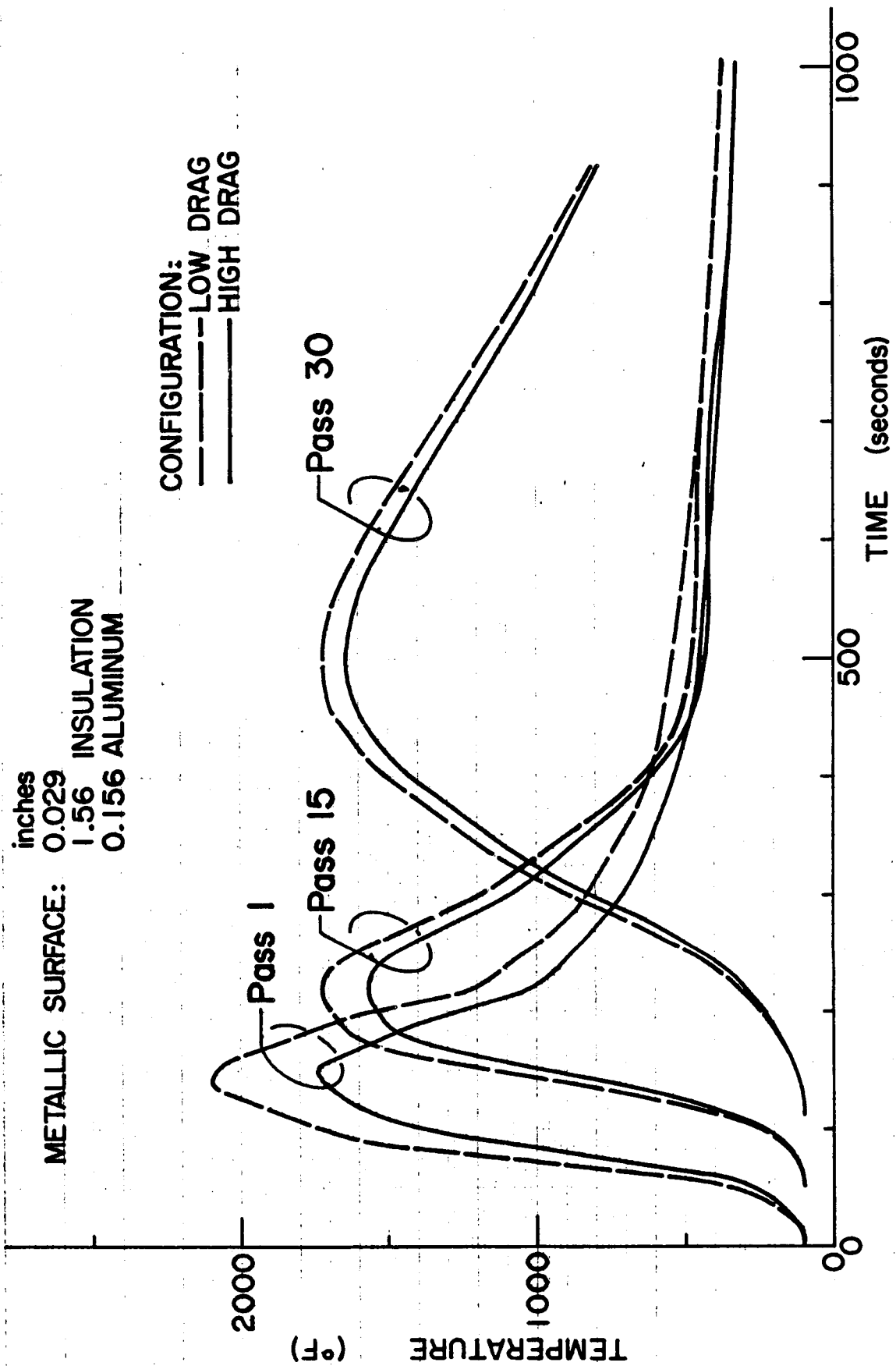
Figure 29 - Temperature Histories for Metallic Heat Shields at Point "B"
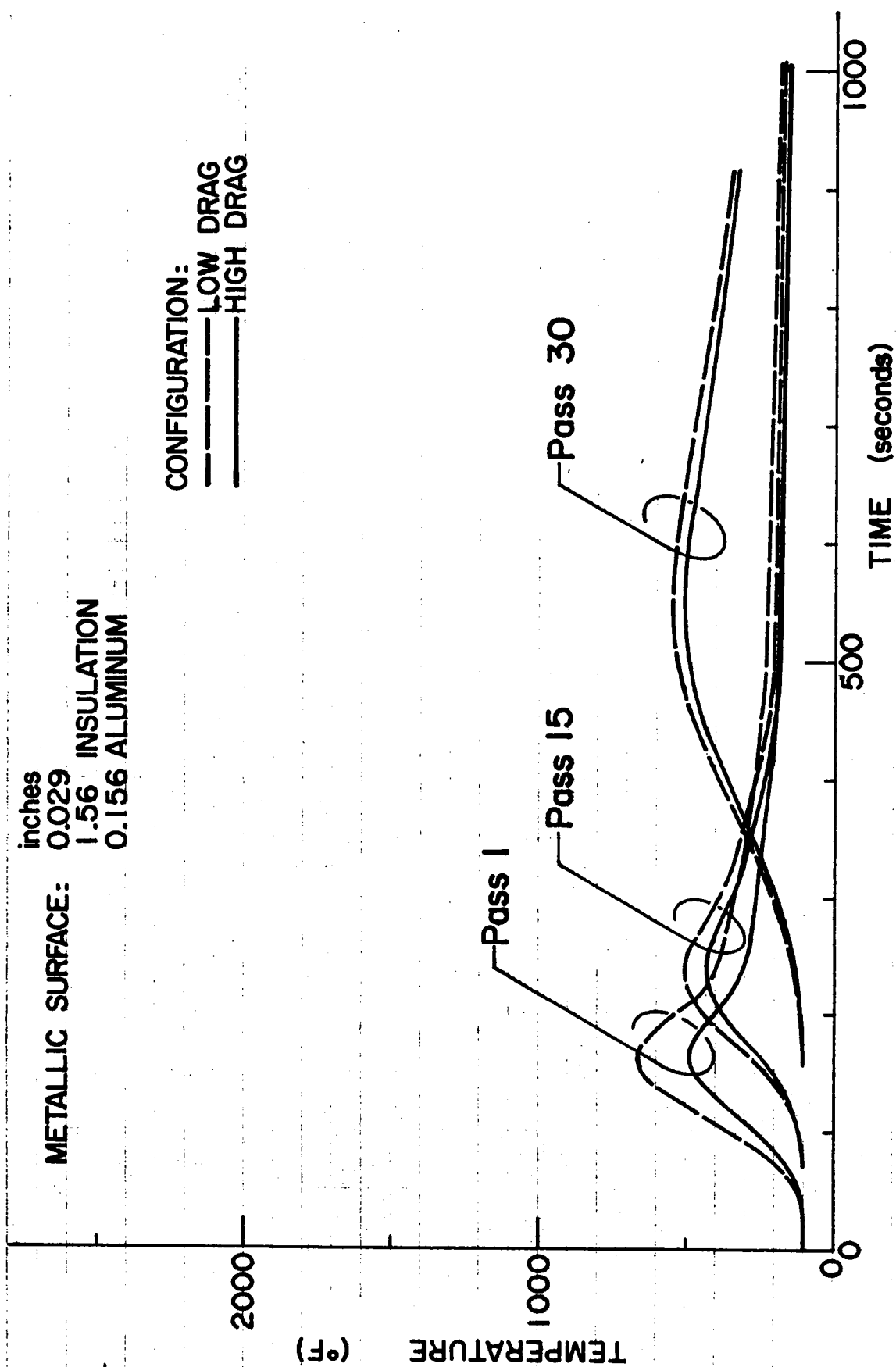
Figure 30 - Temperature Histories for Metallic Heat Shields at Point "C"

PULSE	1	2
$\dot{q}$ (BTU/ft^2-sec)	120 / 27.5	80 / 27.5
t (secs)	50 / 200	90 / 360
H (BTU/lb)	6000 / 3000	4500 / 3000
p (atm)	0.07 / 0.025	0.07 / 0.025
Total Time (secs)	250	450
Q (BTU/ft^2)	11,250	17,100
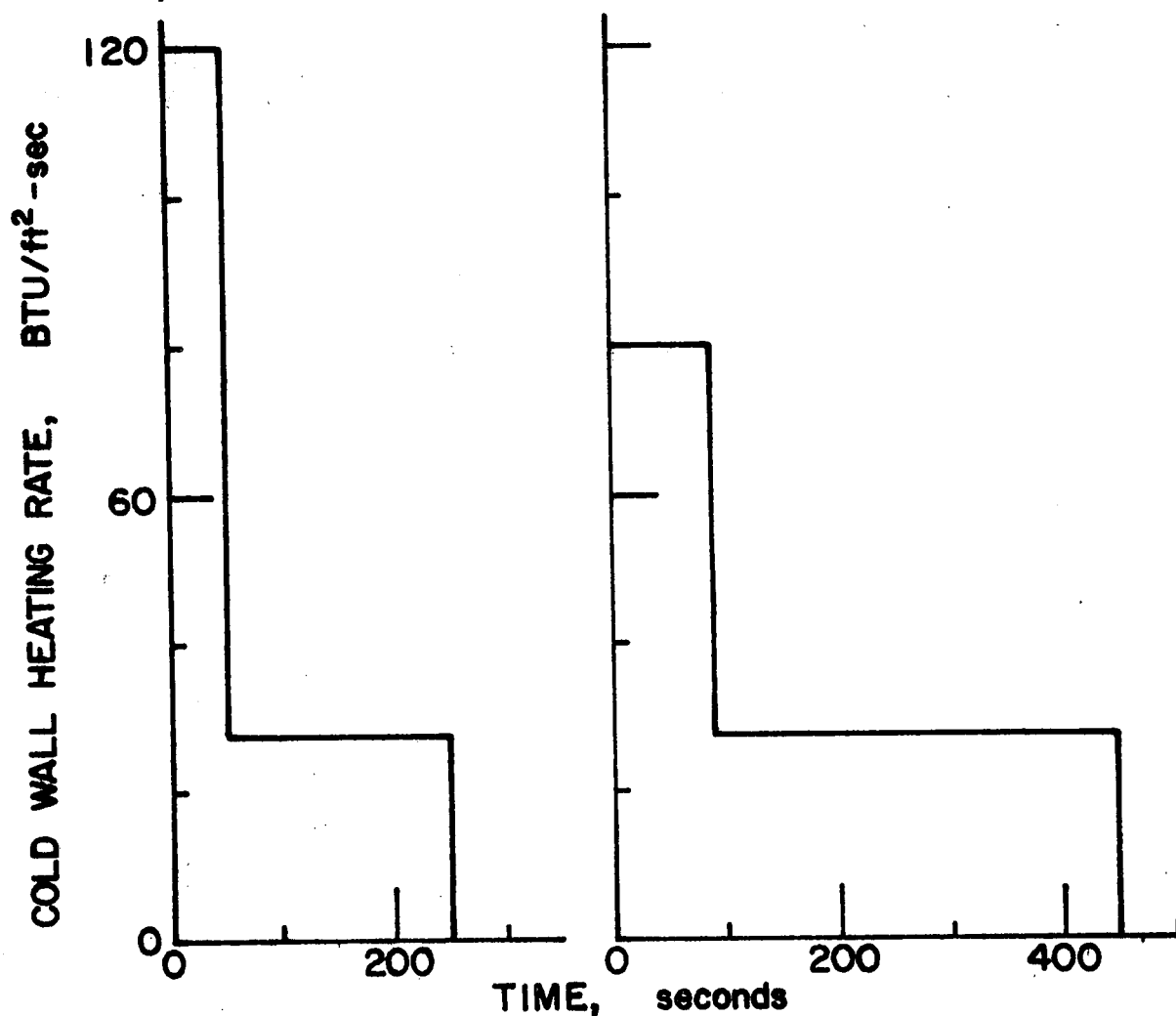
Figure 31 - Two Pass Plasma Arc Test Pulses for Low Drag Configuration

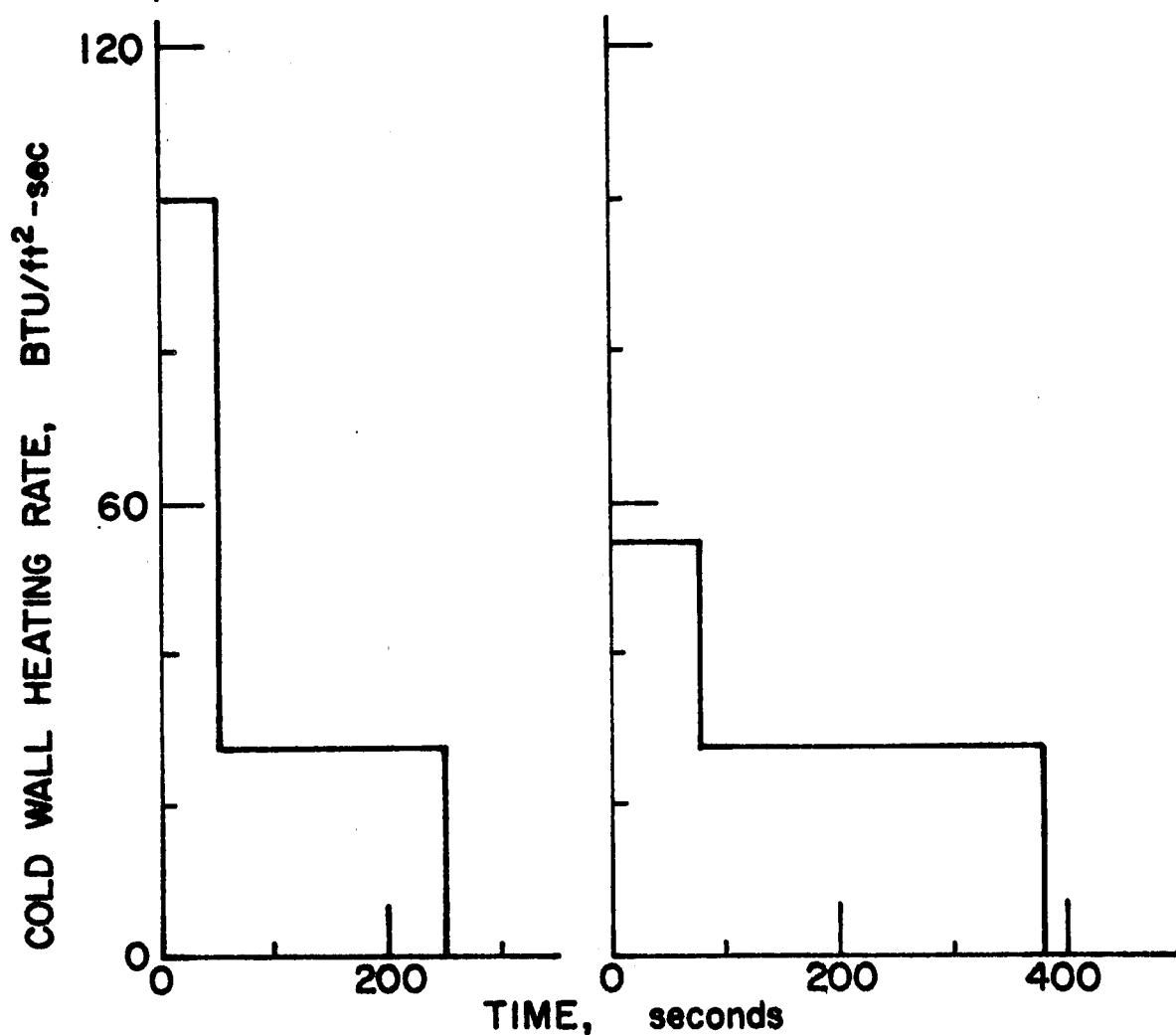| PULSE	1	2
$\dot{q}$ (BTU/ft^2-sec)	80 / 27.5	55 / 27.5
t (secs)	50 / 200	80 / 300
H (BTU/lb)	4500 / 3000	4000 / 3000
p (atm)	0.07 / 0.025	0.07 / 0.025
Total Time (secs)	250	380
Q (BTU/ft^2)	9, 500	12, 650

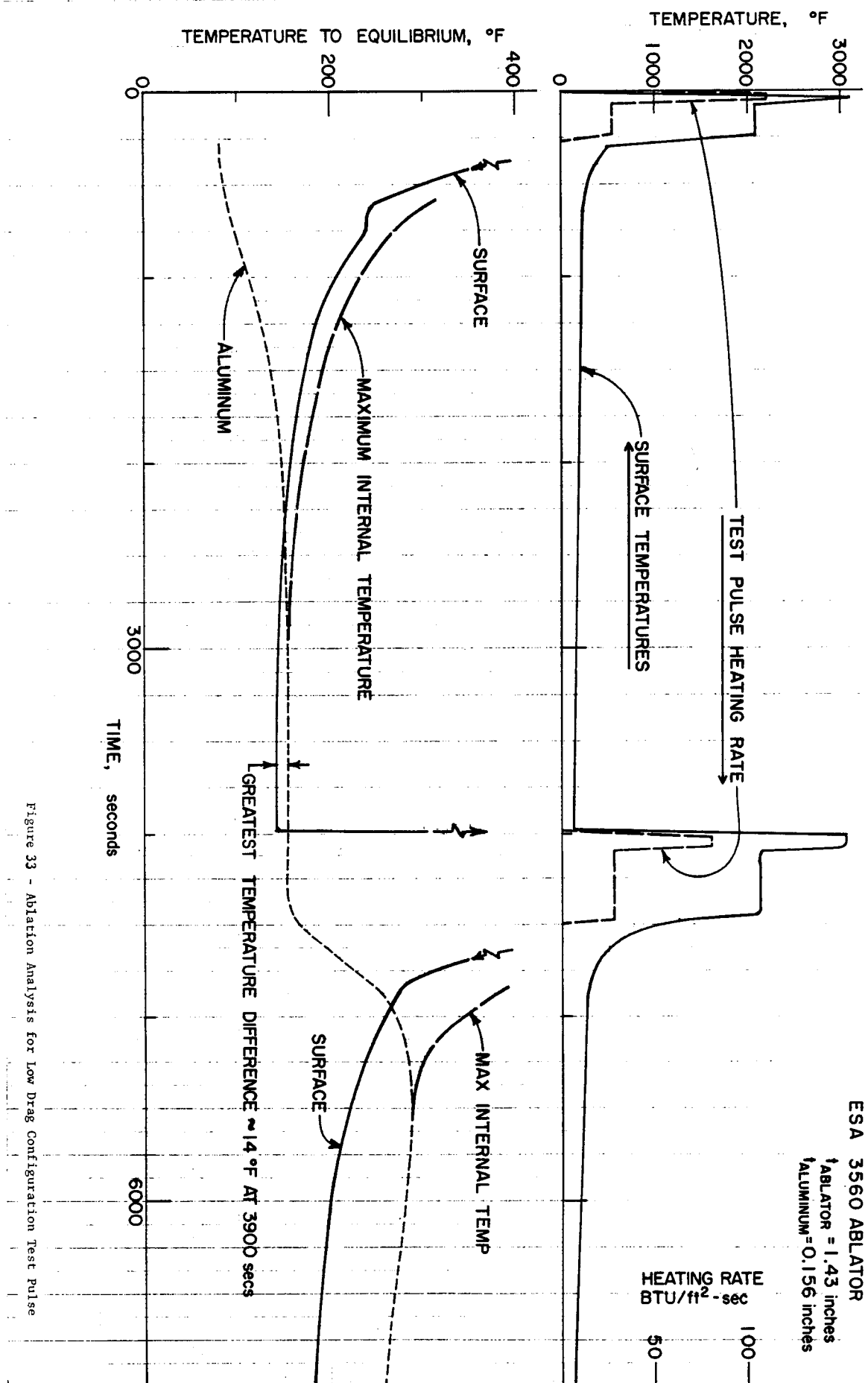Figure 32 - Two Pass Plasma Arc Test Pulses for High Drag Configuration

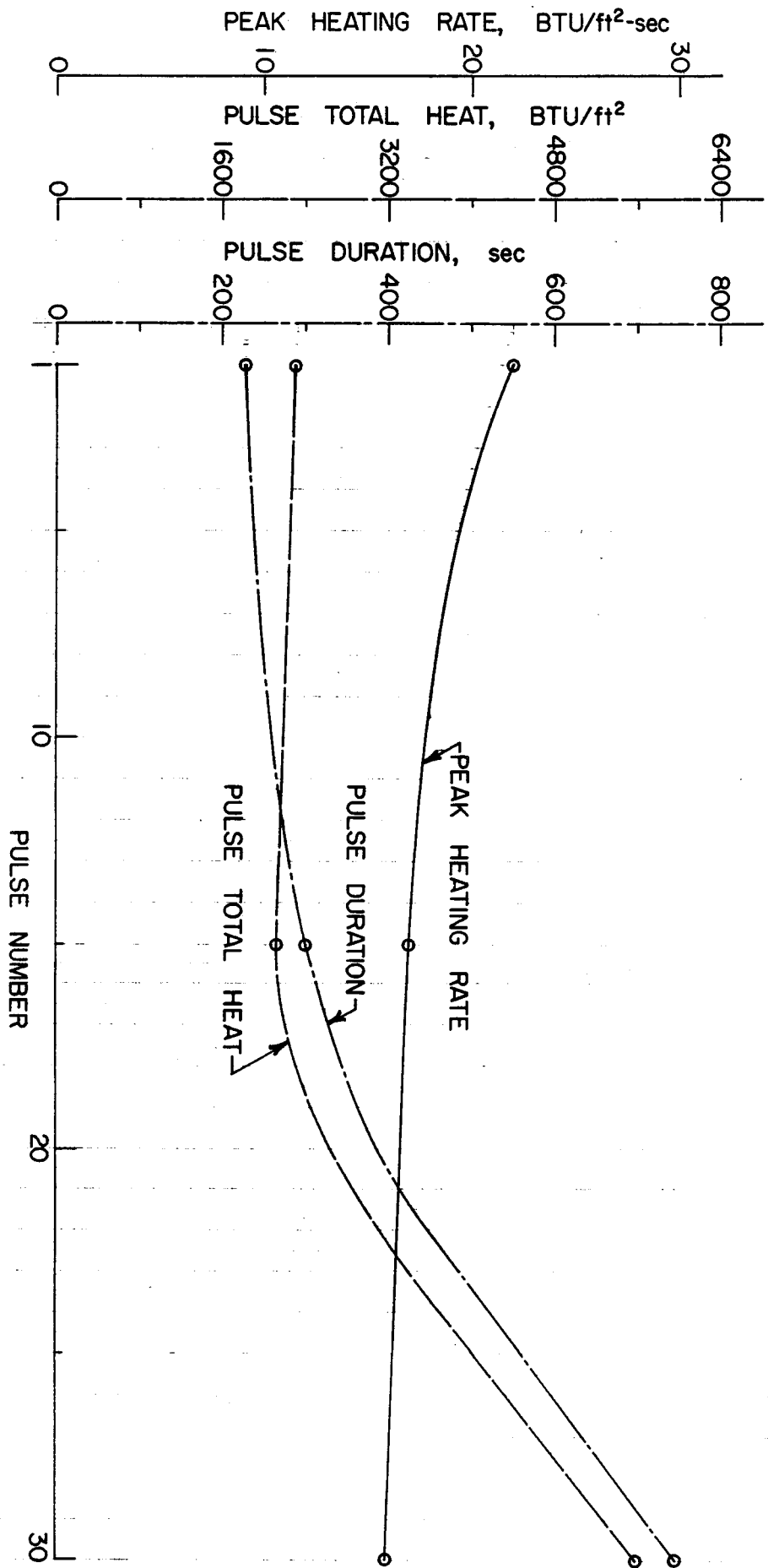Figure 33 - Ablation Analysis for Low Drag Configuration Test Pulse

ESA 3560 ABLATOR
$t_{ABLATOR}$ = 1.43 inches
$t_{ALUMINUM}$ = 0.156 inches

TEMPERATURE, °F

TEMPERATURE TO EQUILIBRIUM, °F

TIME, seconds

HEATING RATE BTU/ft²-sec

SURFACE

MAXIMUM INTERNAL TEMPERATURE

ALUMINUM

SURFACE TEMPERATURES

TEST PULSE HEATING RATE

GREATEST TEMPERATURE DIFFERENCE ≈ 14 °F AT 3900 secs

SURFACE

MAX INTERNAL TEMP

Figure 34 - Heat Pulse Variations with Pulse Number for High Drag Configuration - 30 Pass Entry Trajectory

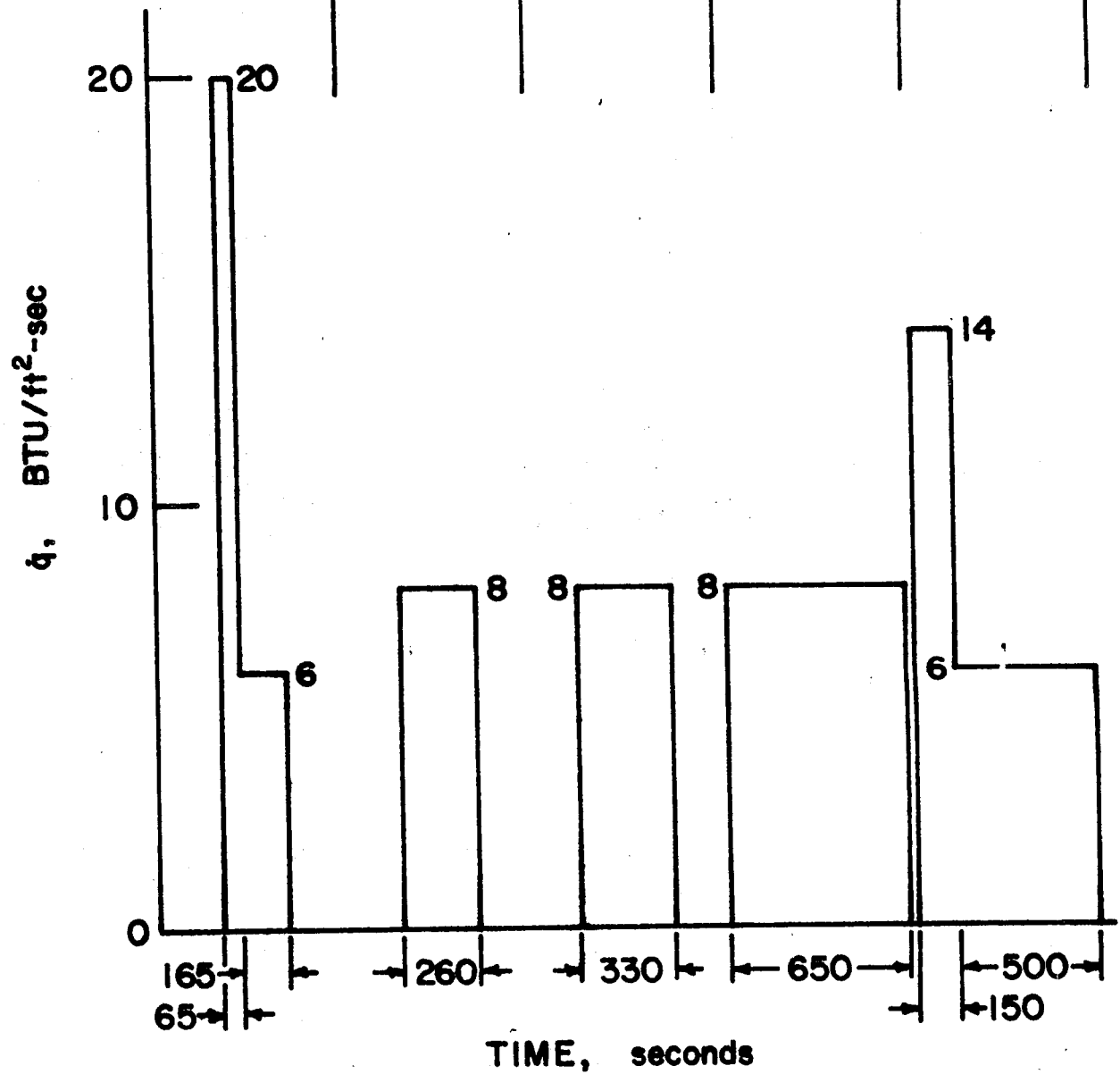| PULSE	1-4	5-14	15-24	25-27	28-30
Q (BTU/ft^2)	2290	2080	2640	5200	5100
P (atm)	$\frac{0.0075}{0.0025}$	0.005	0.005	0.005	$\frac{0.0075}{0.0025}$
H (BTU/lb)	$\frac{5000}{2500}$	3500	3500	3500	$\frac{5000}{2500}$

Figure 35 - Thirty Pass Plasma Arc Test Pulses for High Drag Configuration

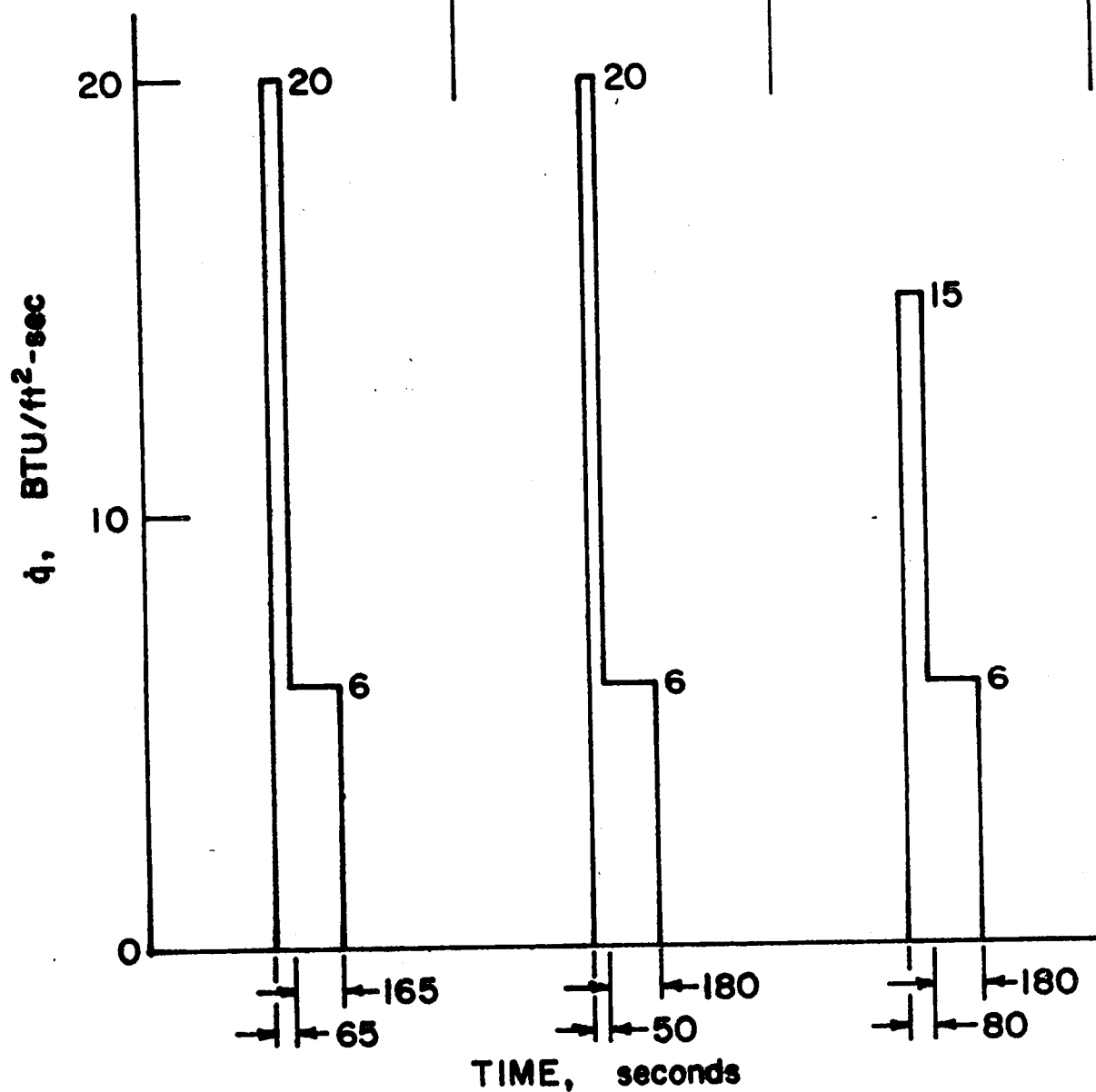| PULSE	1-5	6-10	11-15
Q (BTU/ft^2)	2290	2080	2280
P (atm)	$\dfrac{0.0075}{0.0025}$	$\dfrac{0.0075}{0.0025}$	$\dfrac{0.0075}{0.0025}$
H (BTU/lb)	$\dfrac{5000}{2500}$	$\dfrac{5000}{2500}$	$\dfrac{5000}{2500}$

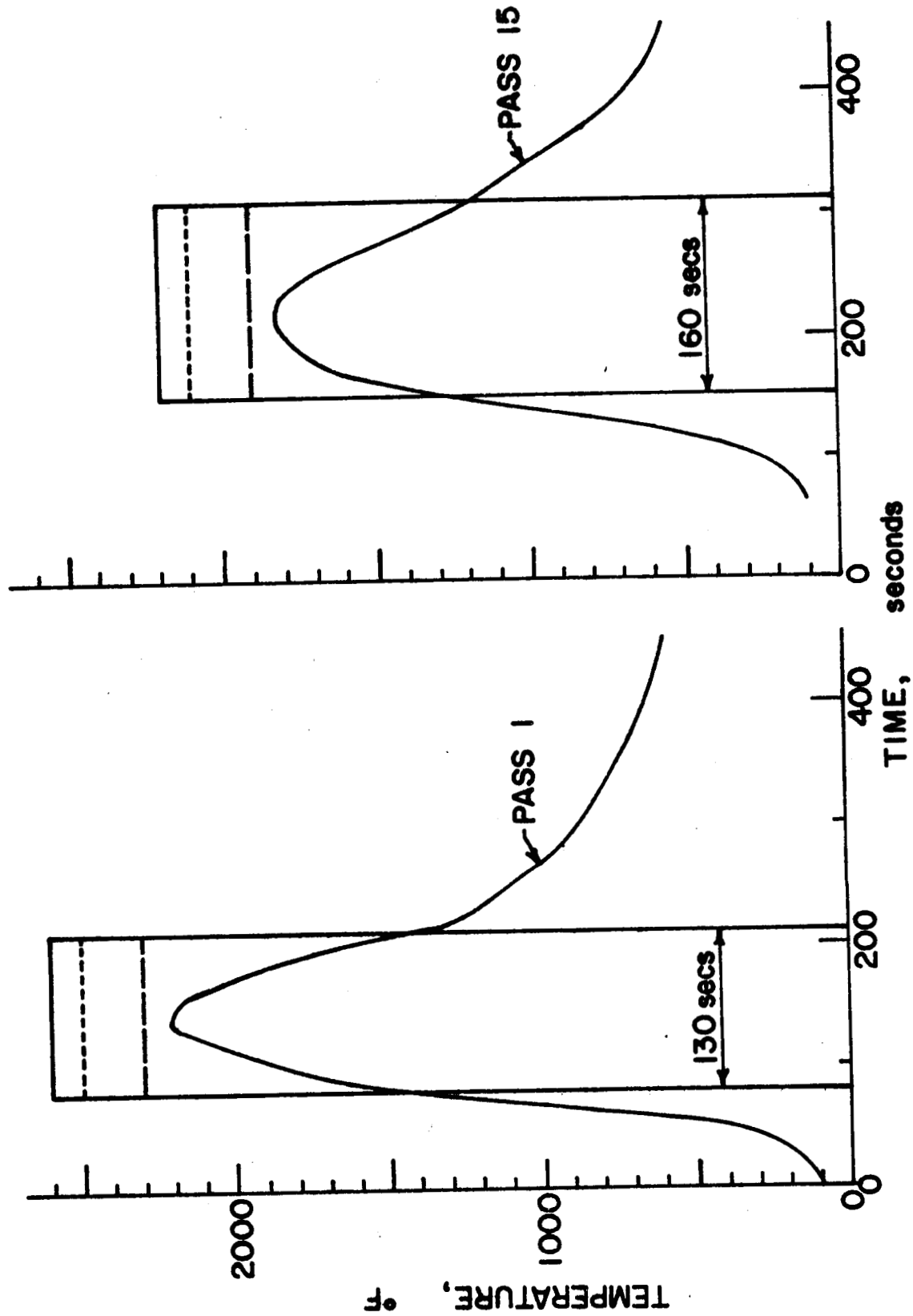Figure 36 - Fifteen Pass Plasma Arc Test Pulses for High Drag Configuration

Figure 37 - Derivation of Plasma Arc Test Pulses for Point "A", Low Drag Configuration, 30 Pass Entry Trajectory
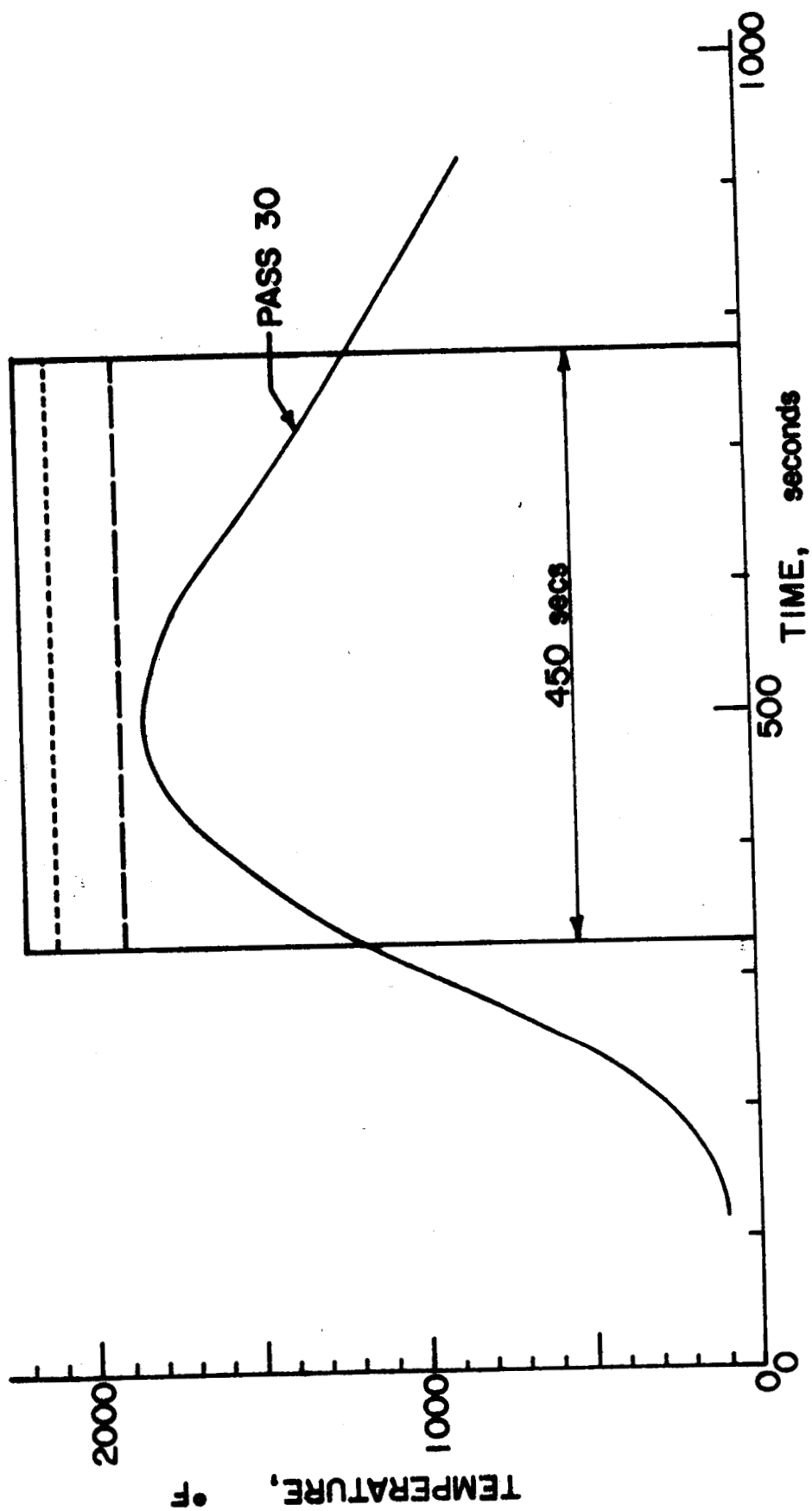
PASS 30

450 secs

TIME, seconds

500

1000

TEMPERATURE, °F

2000

1000

0

0

Figure 37 - Continued

63

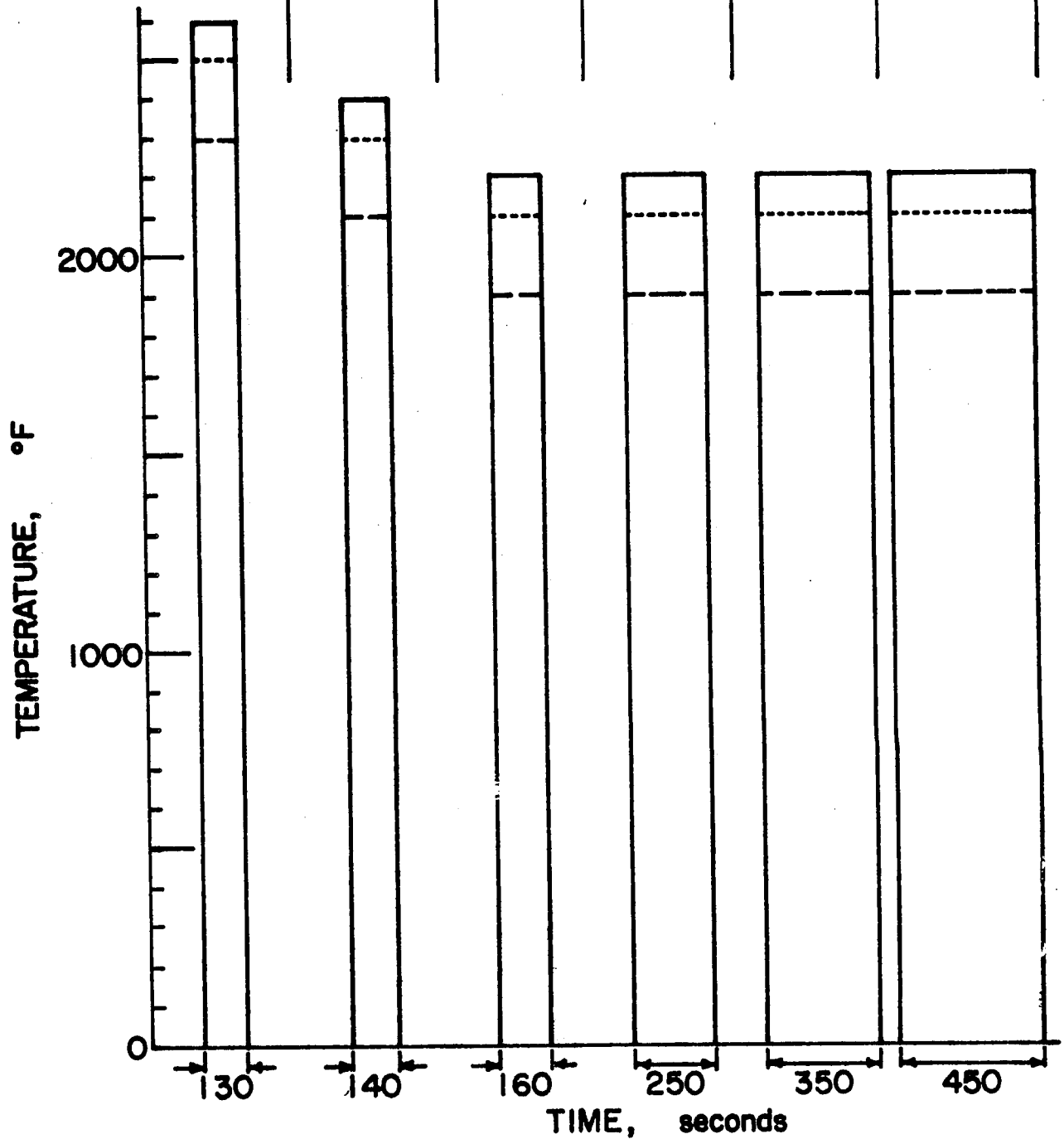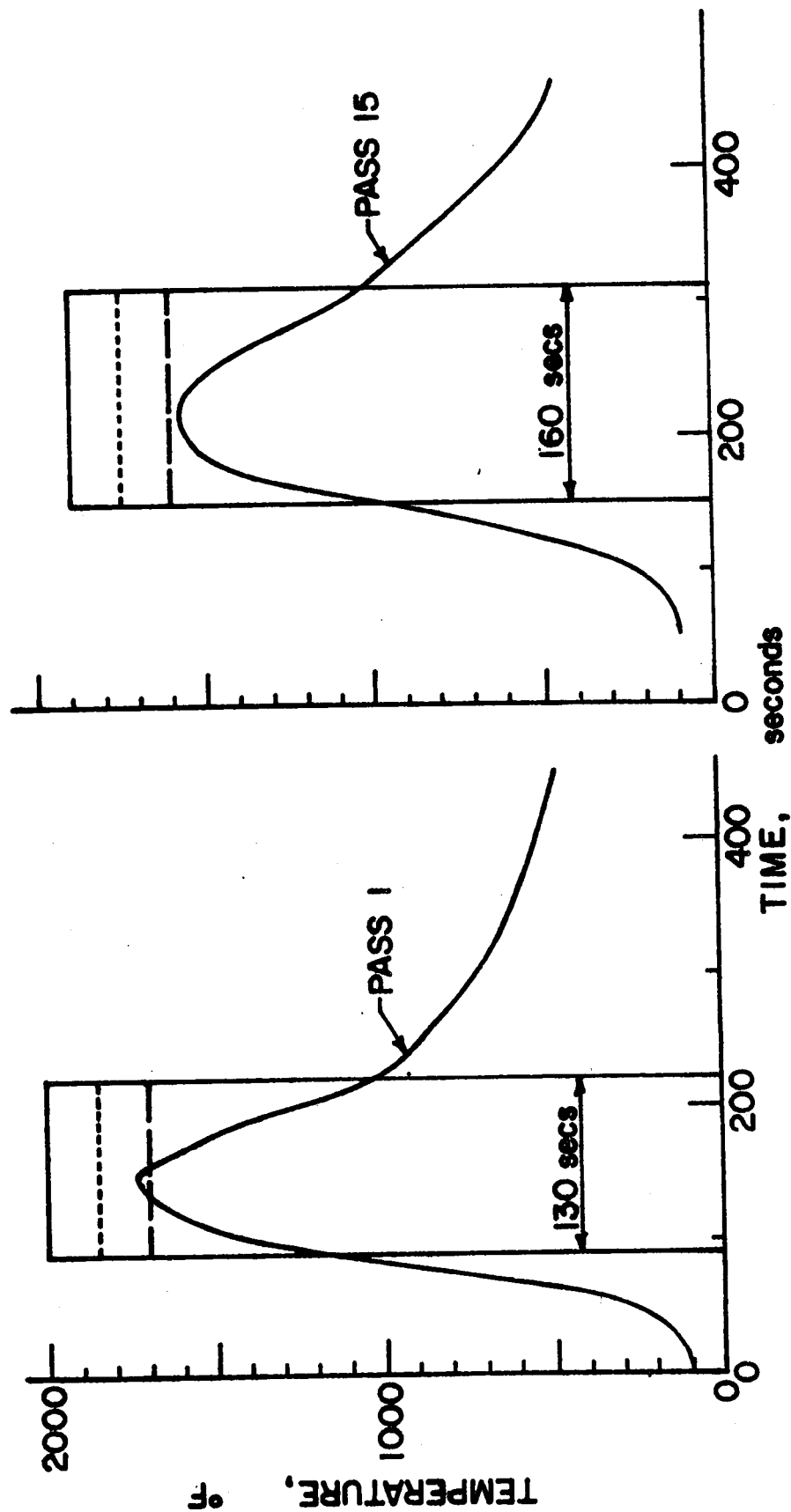| PULSE	1-5	6-14	15-21	22-26	27-28	29-30
MODEL Nº	TEMPERATURE, °F					
1 & 2	2300	2100	1900	1900	1900	1900
3 & 4	2500	2300	2100	2100	2100	2100
5 & 6	2600	2400	2200	2200	2200	2200

Figure 38 - Plasma Arc Test Pulses for Columbium Models

Figure 39 - Derivation of Plasma Arc Test Pulses for Point "B", High Drag Configuration, 30 Pass Entry Trajectory
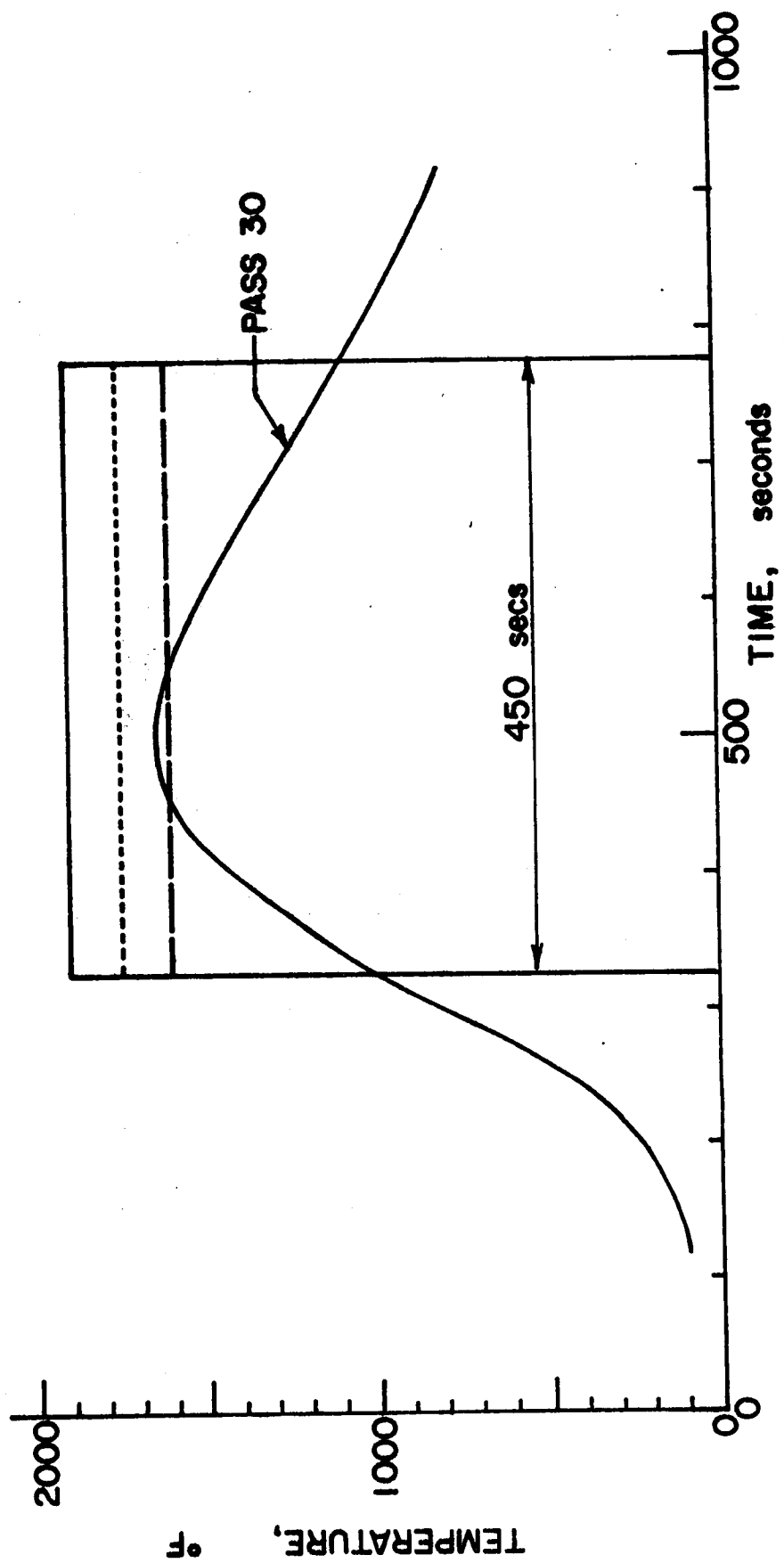
PASS 30

450 secs

TIME, seconds

500

1000

TEMPERATURE, °F

2000

1000

0

Figure 39 - Continued

66

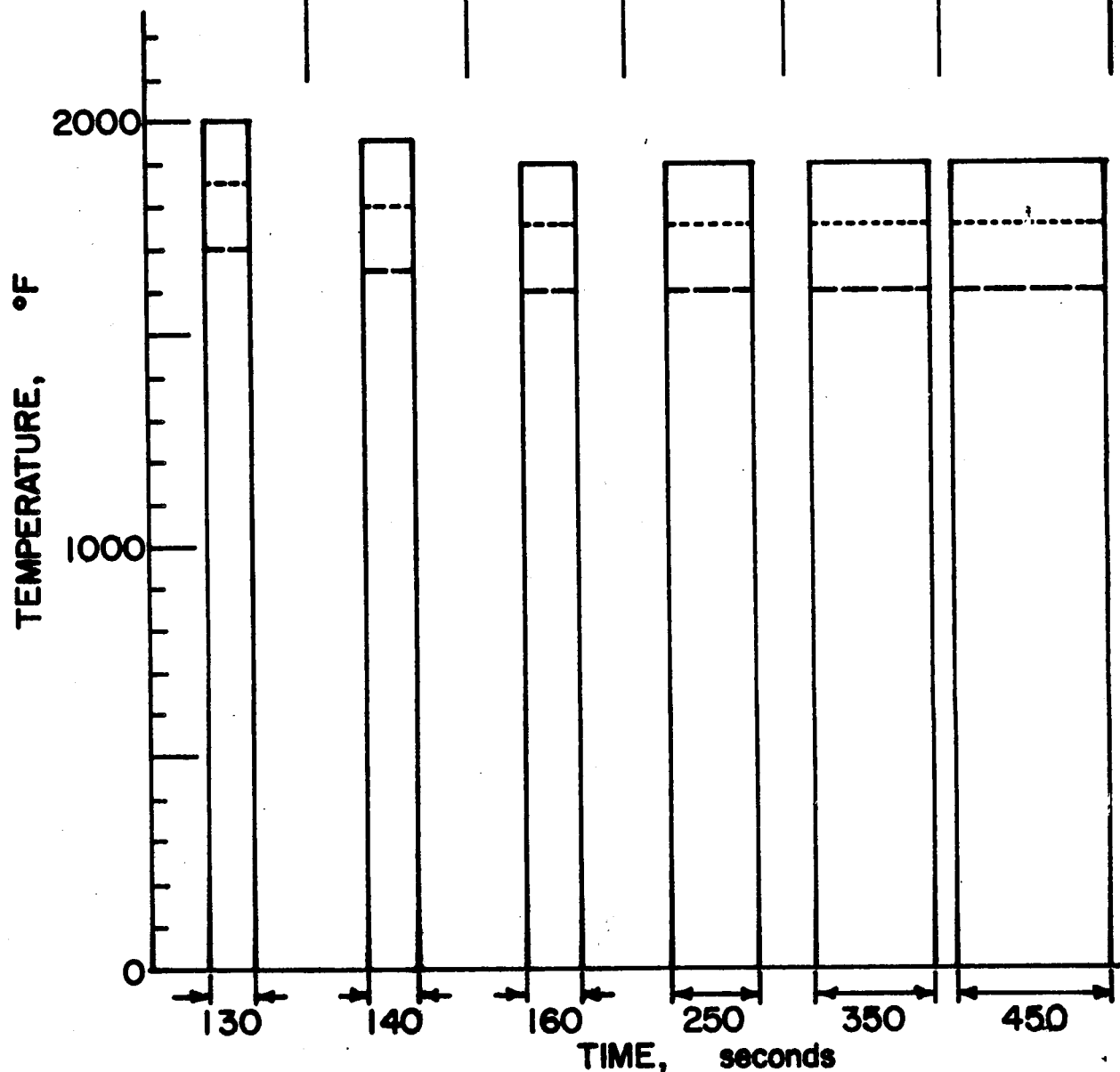| PULSE	1-5	6-14	15-21	22-26	27-28	29-30
MODEL №	TEMPERATURE, °F					
1 & 2	1700	1650	1600	1600	1600	1600
3 & 4	1850	1800	1750	1750	1750	1750
5 & 6	2000	1950	1900	1900	1900	1900

Figure 40 - Plasma Arc Test Pulses for Haynes 188 Models